A Guide to Small Fluorescent Probes for Single-Molecule Biophysics

Mark C. Leake[1,2,3] & Steven D. Quinn[1,3,*]

[1]School of Physics, Engineering and Technology, University of York, Heslington, York, UK. YO10 5DD.

[2] Department of Biology, University of York, Heslington, York, UK, YO10 5DD.

[3] York Biomedical Research Institute, University of York, Heslington, York, UK, YO10 5DD.

* steven.quinn@york.ac.uk

Abstract

The explosive growth of single-molecule techniques is transforming our understanding of biology, helping to develop new physics inspired by emergent biological processes, and leading to emerging areas of nanotechnology. Key biological and chemical processes can now be probed with new levels of detail, one molecule at a time, from the nanoscopic dynamics of nature's molecular machines to an ever-expanding range of exciting applications across multiple length and time scales. Their common feature is an ability to render the underlying distribution of molecular properties that ensemble averaging masks, to reveal new insights into complex systems containing spatial and temporal heterogeneity. Small molecule fluorescent probes are among the most adaptable and versatile for single-molecule sensing applications because they provide high signal-to-noise ratios combined with excellent specificity of labeling when chemically attached to target biomolecules or embedded within a host material. In this review we examine recent advances in small molecule probe designs, their utility and applications, and provide a practical guide to their use, focusing on the single-molecule detection of nucleic acids, proteins, carbohydrates and lipid dynamics. We also present key challenges that must be overcome to perform successful single-molecule experiments, including probe conjugation strategies, identify trade-offs and limitations for each probe design, showcase emerging applications, and discuss exciting future directions for the community.

1. Background

Single-molecule sensing techniques are revolutionizing our understanding of biological systems by enabling the molecular building blocks of life to be studied with extraordinary levels of detail[1], new soft-matter physics relevant to complex processes to be explored and new physics theories to be developed[2]. The last several decades have witnessed an explosive growth in the use of small nanoscale fluorescent probes for investigating biomolecular structure and function under a huge range of experimental conditions. It is now abundantly clear that a capability to measure fluorescence intensity, absorption, quantum yield, spectrum, lifetime, correlation time and anisotropy from single probes *in situ, in vitro,* and *in vivo*, with associated growth in new analytical tools[3], enables researchers to access population distributions that are otherwise hidden by the ensemble average. While X-ray crystallography and electron microscopy tools have, for example, provided important structural details of biomolecular systems, they lack the ability to follow the time-sequence of corresponding dynamics and often miss critical interactions or transient conformations because of the requirement for static, frozen or powdered samples. Fully characterizing biological dynamics and accessing micro-environmental distributions thus requires an ability to follow individual interactions without averaging over all steps in the process, enabling the study of the physics of life in effect one molecule at a time[4]. In this respect, the emergence of single-molecule fluorescence methods has led to transformative insights into cases where static and/or dynamic heterogeneity is present, such as in a biological machine whose properties continuously and dynamically alter over multiple time scales. For all of nature's biomolecules, a variety of chemical and physical events trigger time-dependent conformational switching and interactions, and accessing how they dynamically operate is extremely attractive for researchers across the physical-life sciences interface.

Although some biomolecules contain weakly fluorescing units, for example in proteins the aromatic amino acids (tryptophan, tyrosine and phenylalanine), advances in modern synthesis techniques have enabled highly emissive fluorescent probes to be chemically tagged to biomolecular structures with high specificity. Since the earliest detection of single pentacene molecules at low temperatures[5, 6], techniques which enable fluorescence detection from small molecular probes tagged to target biomolecules under physiological environments have developed rapidly and been applied extensively, as approximated by the abundance of research papers with "single-molecule fluorescence" in the article. Although this is clearly a simple analysis, the number of such papers per year, shown in **Figure 1a**, demonstrates that the field has more than doubled in size since a similar analysis was carried out over a decade ago[7].

The visualization of these single-molecule fluorescent probes has primarily enabled the localization and diffusion of single biomolecules to be observed directly[8], but more complex interactions such as protein dynamics[9-11], folding kinetics[12-14], and stoichiometry and kinetics of functional enzymes and molecular machines inside living cells[15-18], can also now be followed through changes to their spectroscopic fingerprints. Their utility has also extended to environmental sensing, enabling the organisation and architecture of lipid membranes[19-21] and signalling complexes on the surfaces of living cells[22, 23] to be explored. In addition to aiding visualization, these probes have become indispensable to the modern researcher because they also provide dynamic information concerning the quantity of the localized biomolecule in diffraction-limited volumes.

Another powerful application rests in Förster resonance energy transfer (FRET) experiments[24], where donor and acceptor probes are tagged to key molecular components

of a biological system, and changes in their fluorescence properties (intensity and lifetime) report quantitatively on their separation distance with a ~1-10 nm sensitivity[25]. Widely considered as a spectroscopic nano-ruler, FRET has become a popular workhorse technique for identifying and characterizing real-time conformational changes within single nucleic acids[26-28] proteins[29] and enzymes[30], and recent probe developments[25] have seen it combined with integrative modelling, giving rise to a new field of quantitative structural biology[31-33]. The development of non-fluorescent acceptors (so-called Black Hole Quenchers) have also complemented this area, enabling single-colour FRET experiments to quantitatively report on conformational fluctuations[34, 35].

Fluorescent probes have also found utility in experiments tailored towards sub-millisecond temporal resolution[36], and they are providing new opportunities for linking heterogeneous transfer dynamics with thermal fluctuations in biological structures[37]. Another interesting application is the real-time measurement of orientations of single molecules using polarized emission. Here, the probes emit polarized light along the axis of their transition dipole moments and if, for example, the polarized fluorescence emission intensity is measured as a function of the excitation polarization, then this can allow for quantification of the probe's local orientation and rotational characteristics[38]. The methodology has already been applied to the understanding of intercalators[39], probing biomolecular conformation under tension[40, 41], following rotational dynamics within membranes[42] and has facilitated investigations into tilting during processive motility[43], with new methods capable of correlating fluorescence polarization with super-resolved localization precision[44].

As demonstrated in **Figure 1b**, the demand for, and applications of, small molecule fluorescent probes is growing considerably. In nearly all applications, the combination of photon statistics and physical laws quantitatively describes the behaviour of single tagged biomolecules at work, enabling researchers to pinpoint key pathways and mechanisms which underpin the physics of life[4]. This ability undoubtedly places single-molecule fluorescence techniques at the forefront of the physical-life sciences interface[45].

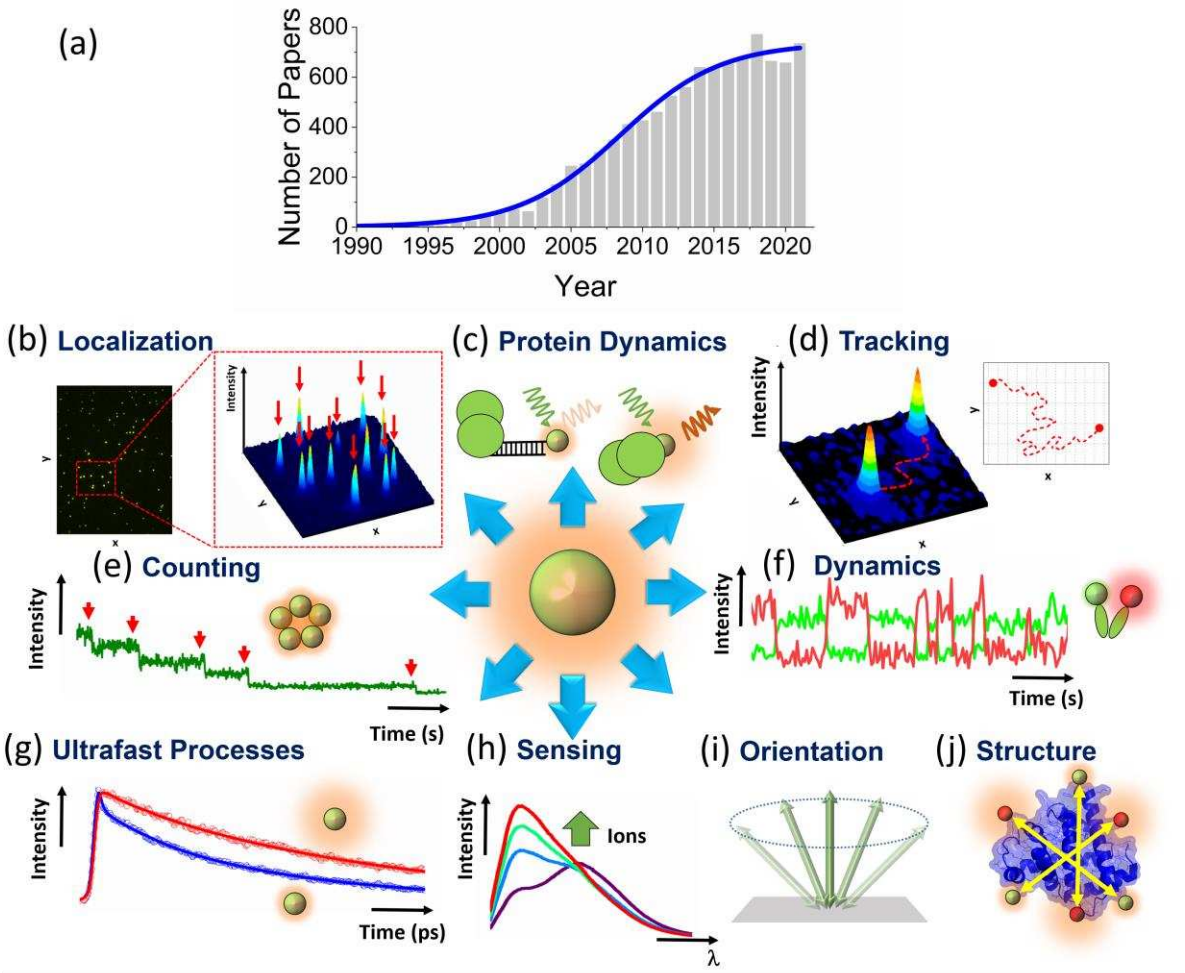

Figure 1. Small molecule fluorescent probes enable quantification of biological interactions and dynamics. (a) The number of papers indexed in the PubMed database with "single molecule fluorescence" in the article illustrates the growth of the field. (b-j) Single-molecule fluorescence techniques provide quantitative information on a wide-range of parameters. For example, (b) by following raw image acquisition from small molecule fluorescent probes, the intensity profile of each molecule may be modelled to reveal the probe's location with nanometre precision if the number of emitted photons per probe is typically $>10^7$. (c) The binding of a protein to a small molecule probe may in some cases lead to fluorescence enhancement. The protein-induced enhancement is a particularly powerful approach for probing protein dynamics upon interaction with nucleic acids. (d) By capturing images as a function of time, 2D correlation maps documenting all detected probe locations can be used for particle tracking. (e) Under continuous excitation, each fluorescently-tagged sub-unit within a complex photobleaches causing a stepwise fluorescence decrease in approximately equal magnitude steps. The number of active fluorophores, and therefore number of photobleaching steps, yields the complex stoichiometry. (f) Anti-correlations in the fluorescence time traces of donor- (green) and acceptor- (red) labelled complexes enable nanoscale molecular dynamics to be accessed via FRET. (g) Fluorescence decay curves obtained via time-correlated single photon counting techniques reveal lifetime distributions and interconvesion rates reflecting biomolecular conformations and environments. (h) Fluorescence emission spectra of various probes shift in response to changes in the local biomolecular environment, enabling accurate determination of, for example, local ion concentrations. (i) Polarization microscopy enables rotational and orientational behaviours to be extracted from single probes. Here, the orientation of a probe's dipole moment rotating about an axis can be determined; the dipole is only efficiently excited when it rotates through the axis of the excitation polarization. (j) FRET analysis captures the structure of single biomolecules, with distance errors reported to be as low as only a few percent.

This review highlights advances in the development of fluorescent probes for single-molecule imaging and spectroscopy applications, focusing on those that can resolve spatial and temporal dynamics of individual biomolecules at work. As the number of successful fluorescent reporters increases, several design trends and considerations are becoming apparent. We highlight the most robust and adaptable of these designs and showcase their utility in the next-generation of single-molecule experiments.

2. Emerging Small Molecule Fluorescent Probe Designs

Single-molecule fluorescence studies generally make use of extrinsic probes that are either specifically linked to a target biomolecule, non-specifically intercalated into its structure, or embedded within a host matrix. They span the visible spectrum, as well as extending into the ultraviolet and near-infrared, and can be coupled to almost any biomolecule of interest, from nucleic acids and proteins, to carbohydrates, cholesterols and lipids. A huge variety of probes now exist, and each has its own unique photophysical properties. However, great care must be taken to choose an appropriate label for each application since it is vital to maximize the signal-to-noise ratio detected from each individual molecule. Selection of a suitable probe with robust enough photophysical properties is thus a critical first step in the experimental design process.

In general, the probes should satisfy four major conditions. First, they should display excellent photophysics within the biomolecule's local environment. They should be water soluble, have an ability to strongly absorb excitation photons (extinction coefficient, ε, > 50,000 $M^{-1}cm^{-1}$) and be sufficiently emissive (quantum yield, ϕ, > 0.1) for the desired spatio-temporal resolution[24]. Additionally, the probes should not aggregate in solution and remain photoactive across the duration of the measurement time window (photobleaching quantum yield, $\phi_{pb} < 10^{-6}$-10^{-7})[46, 47]. Second, they should contain a linker for high specificity or demonstrate ease-of-delivery towards the biomolecule of interest. Third, they must also minimize any putative impairment to biological function due to steric hindrance effects. This is often carefully checked by comparing the activity of the labelled species with its unlabelled counterpart. Finally, and in the context of ratiometric FRET-based measurements, the chosen fluorophores should have large spectral separation between their emissions, have similar quantum yields and must not exhibit time-dependent spectral shifts or intensity fluctuations[24, 48]. In this section, we focus the discussion on the most popular small molecule fluorescent probe designs which satisfy these conditions, including recent advances, emerging trends, their use and relative performance.

2.1 Organic Dyes

Organic dyes are among the smallest in length scale (< 1 nm) and most adaptable of all small molecule probe designs. When properly positioned, they are generally considered among the least invasive and perturbing. Their structure facilitates electron delocalization through a conjugated π-electron system, enabling the molecule to act as an efficient electric dipole. Organic dyes used for single-molecule fluorescence studies typically absorb and emit across the visible region of the electromagnetic spectrum though due to issues with photostability with dyes that absorb below 450 nm, and limitations regarding detection sensitivity at infrared wavelengths, most single-molecule fluorescence experiments involve organic dyes that cover the 480-750 nm window[49, 50].

Organic dyes are broadly classified into six major families: the cyanines, oxazines, boron-dipyrromethenes, perylenes, diketopyrrolopyrroles and xanthenes, with the latter consisting of particularly popular fluorescein and rhodamine derivatives such as the ATTO dyes.

The cyanines have the general structure shown in **Figure 2a** and have found most utility for single-molecule applications involving proteins. Their lipophilic properties meant that they initially found utility as membrane stains, but sulfonated indocarbocyanine derivatives including Cy3, Cy5 and Cy7 (**Figure 2d-f**) are now widely used for biomolecular labelling. The cyanines are named according to the number of carbon atoms between the indoline moieities with the longer polymethine chains corresponding to longer emission wavelengths. In this example, Cy3, Cy5 and Cy7, exhibit peak emission at 568 nm, 652 nm and 755 nm, respectively. While their quantum yields are typically lower than many other organic dyes (ϕ_{Cy3} ~ 0.31; ϕ_{Cy5} ~ 0.27; ϕ_{Cy7} ~ 0.2), their high extinction coefficients (ε_{Cy3} ~ 150,000 $M^{-1}cm^{-1}$; ε_{Cy5} ~ 250,000 $M^{-1}cm^{-1}$; ε_{Cy7} ~ 199,000) $M^{-1}cm^{-1}$position them among the brightest[51].

Longer-chain dialkylcarbocyanines such as DiO, DiI and DiD are often employed as membrane stains for live-cell[52], fixed tissue[53] and model-membrane[54] imaging. Due to their excellent lipophilic properties, incubation of biological membranes with solutions containing the probes for only a few minutes is sufficient to achieve uniform labelling via lateral diffusion (**Figure 3a**). In this way high probe density is often obtained, with minimal reported effects on cell viability or physiology[52, 55]. An important point is that they do not tend to transfer from labelled to unlabelled membranes, except in the case of targeted fusion[56]. The spectral characteristics of the dialkylcarbocyanines are determined by the heteroatoms in the terminal ring systems and length of the connecting bridge, as opposed to the chain length. DiO, for instance, absorbs strongly at 484 nm with peak emission at 501 nm, while DiI and DiD absorb and emit at 549/644 nm and 565/665 nm, respectively (**Figure 3b**). Much like the short-chain derivatives, the longer chains also have high extinction coefficients (ε_{DiO} ~ 140,000 $M^{-1}cm^{-1}$; ε_{DiI} ~ 148,000 $M^{-1}cm^{-1}$; ε_{DiD} ~ 193,000) and comparable excited state lifetimes (~ 1 ns), though their quantum yields tend to be somewhat lower (~0.07)[57, 58]. Such probes offer a chance to probe the local dynamics and curvature of lipid bilayers via measurement of their rotational time trajectories[42, 59]. Both DiI and DiD, for example, have two hydrocarbon tails that mimic phospholipid tails, and their transition dipole moments lie along the plane of the membrane; thus they are excellent candidates for probing rotational motions.

Unlike the dialkylcarbocyanines, lipophilic aminostyryl probes such as DiA and 4-Di-10-ASP undergo substantial spectral shifts when incorporated within a membrane environment, and as such have also been employed for membrane staining, despite comparatively broad absorption and emission spectra (**Figure 3c**)[60]. Derivatives including FAST DiI, in which the saturated tails have been replaced with diunsaturated alkyl groups offer accelerated membrane diffusion and staining, while sulfonated, thiol-reactive variants, including CM-DiI are suitable for staining after permabilization[61]. Through FRET-based experiments, in which energy is transferred from membrane-embedded donors to acceptors (**Figure 3a**), the incorporation of such dyes into model vesicles at relatively low molar percentages (~0.1 %) has been used to monitor vesicle fusion through lipid mixing assays[58, 62] and to reveal solubilisation mechanisms and kinetics[21, 63, 64].

While the cyanines represent one of the most versatile and adaptable of all small molecule probe designs, they are subject to photo-induced oxidation even in the presence of low levels of oxygen. As such, without the presence of oxygen scavengers in the local

fluorophore environment, the dyes are subject to fast photobleaching rates, which often limits their use for long-term imaging[65].

The xanthenes represent another widely used group of probes, with the most popular being fluorescein- and rhodamine-based (**Figure 2b**). Synthesis is typically achieved via a simple condensation reaction, though traditional approaches in this regard were compatible only with the simplest functional groups. As a consequence, Pd-catalyzed cross-coupling strategies beginning from simple fluorescein emerged, giving rise to a series of organic dyes commonly referred to as the Janelia Fluor (JF) dyes[66]. The JF probes contain four-membered azetidine rings and have larger quantum yields and enhanced photostability relative to those reported for classic rhodamines and cyanines[67]. JF 549 ($\varepsilon_{JF\ 549}$ = 101,000 $M^{-1}cm^{-1}$, $\phi_{JF\ 549}$ = 0.88) (**Figure 2j**) which emits at 571 nm, has, for example, found particular utility in live-cell applications[68, 69]. Replacing the xanthene oxygen in JF 549 with a quaternary carbon gives rise to JF 648 ($\varepsilon_{JF\ 648}$ = 152,000 $M^{-1}cm^{-1}$, $\phi_{JF\ 648}$ = 0.54) with emission centred on a wavelength of 631 nm[70]. Longer emission wavelengths of 664 nm (for example JF 646; $\varepsilon_{JF\ 646}$ = 152,000 $M^{-1}cm^{-1}$, $\phi_{JF\ 646}$ = 0.54) are also available through Si-Rhodamine synthesis, while shifts to shorter wavelengths have been achieved by replacing the azetidine group with an oxygen atom[71, 72]. Much like the cyanines, the xanthenes also suffer from limited photostability, though factors such as solubility, membrane permeability, cell compartmentalization and aggregation are dependent on the specific chemical structure of the probe and must be accounted for on a case-by-case basis[51]. Nevertheless, their adaptability and comparable brightness to the cyanines also mean that they are commonplace among single-molecule research labs.

The boron-dipyrromethenes (BODIPYs) represent a relatively new class of probe. Much like the cyanines and xanthenes, they too exhibit narrowband absorption and emission spectra, but in contrast they have significantly higher quantum yields, often approaching unity. For example, the quantum yields of BODIPY 581/591, BDP TR, BDP TMR and BDP FL are 0.83, 0.90 and 0.95 and 0.97, respectively. However, strong intramolecular hydrogen bonding between hydroxyl and formyl groups within the BDP structure introduce backbone rigidity, and this leads to relatively small Stokes shifts of only a few nanometres[73]. BODIPY FL (**Figure 2g**) is a common substitute for fluorescein but with peak absorption and emission at wavelengths of 503 nm and 509 nm, respectively, only a 6 nm window exists for resolving the excitation and emission. On the other hand, BODIPY TMR (**Figure 2h**), a derivative synthesised to match tetramethylrhodamine fluorescence, has peak absorption and emission at wavelength of 545 nm and 570 nm, offering improved flexibility. Despite favourable photophysical properties associated with the free dye in solution, BDP derivatives have reportedly suffered from reduced brightness upon conjugation to proteins, which ultimately places a constraint on single-molecule sensitivity[74]. The relatively high hydrophobicity associated with BODIPYs also means care must be taken to ensure minimal non-specific adhesion[75]. Despite these concerns, BODIPYs have found utility in single-molecule applications involving protein folding[76, 77] and recently, photoswitchable versions have found utility in efficient FRET-based measurements[78-80].

Most organic dyes are available with functional groups for bio-conjugation, and many have been modified to include side chains and/or double bonds at specific locations in order to reduce flexibility, minimize Cis-Trans isomerization and enhance the quantum yield. Cy3, for example, is capable of undergoing isomerization around the polymethine group and this can lead to spectral shifting and photoblinking. By incorporating three six-membered rings into its backbone, the derivative (Cy3B) is conformationally locked and exhibits a 4-fold relative enhancement in quantum yield[46]. Similarly, organic dyes with additional sulfo-groups help improve solubility, while charged sulfonate groups help decrease dye

aggregation[48]. For these reasons, organic dyes are also interchangeable. Cy5, for instance, is spectrally similar to Alexa Fluor 647 (**Figure 2k**) but displays poor relative photostability. The incorporation of sulfonic acid groups into the Alexa Fluor 647 structure provides higher levels of solubility by comparison[81].

While the spectral characteristics of many organic dyes are similar, they also have many other unique attributes, and their performance must be carefully scrutinised for each purpose. For example, ATTO647N represents one of the most emissive and photostable red-emitters and has been used to achieve high spatial accuracy in super-resolution and localization experiments[82-84]. However, it is comparatively hydrophobic when compared with many other organic dyes and can, depending on the environment, exhibit substantial spectral shifts[24].

Most organic dyes have found utility in protein and nucleic acid labelling, however to date there have been only a handful of reports on the single-molecule detection of carbohydrates. While the imaging of single Alexa Fluor 488 (**Figure 2i**) labelled heparan sulfate disaccharides encapsulated within lipid vesicles has been reported[85], as has the detection of Alexa Fluor 647 tagged monosaccharides[86, 87] and Cy7-labelled maltose[88], this is clearly an area which demands further development, not least because carbohydrates underpin a wide-class of vital cellular functions.

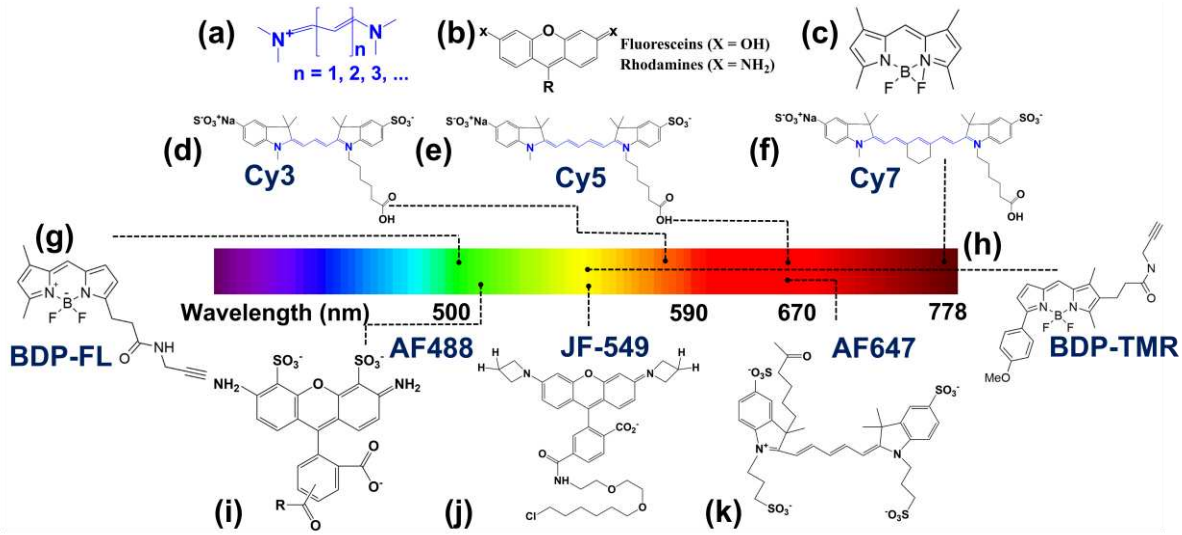

Figure 2. Chemical structures of commonly used organic dyes for single-molecule sensing applications. The general chemical structures of (a) cyanines, (b) fluoresceins and rhodamines and (c) BODIPYs. Also shown are the chemical structures of (d) Cy3, (e) Cy5, (f) Cy7, (g) BDP-FL, (h) BDP-TMR, (i) AF488, (j) JF-549 and (k) AF647. Dotted lines indicate the peak emission wavelength of each probe design.

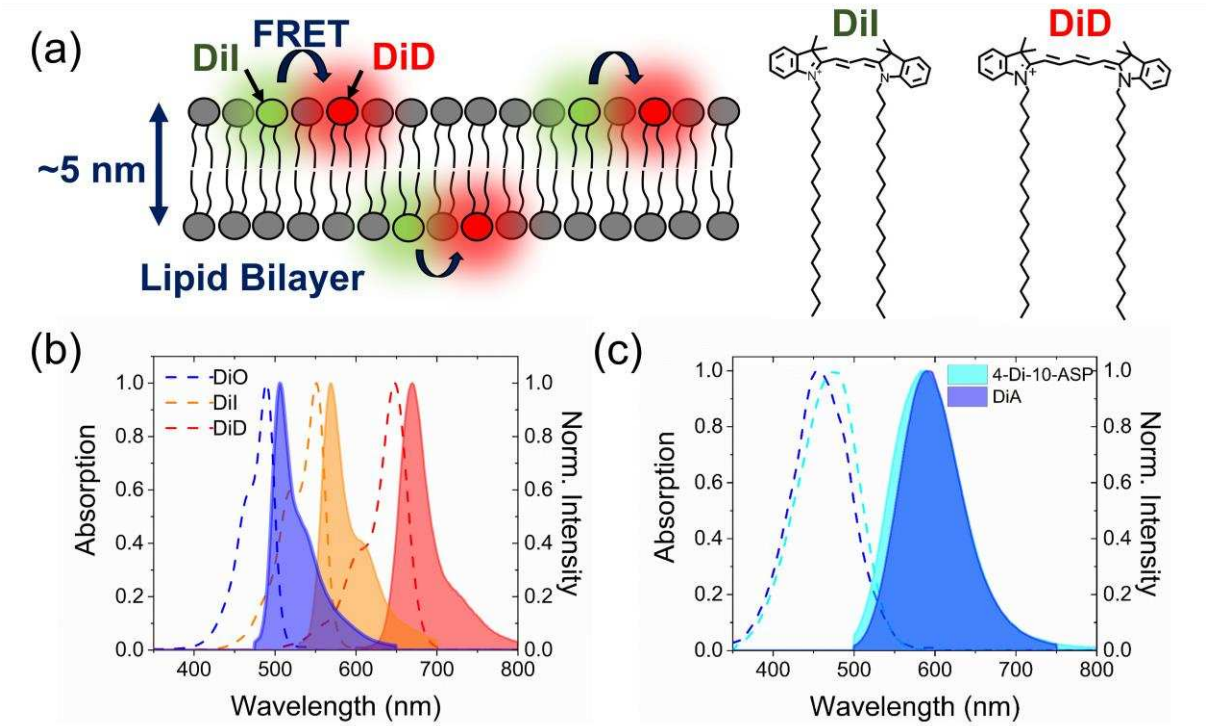

Figure 3. Spectral characteristics of lipophilic membrane stains. (a) Schematic illustration of a lipid bilayer stained with the FRET pair DiI and DiD (left panel). The structures of DiI (~2.1 nm long) and DiD (~2.0 nm long) (right panel), contain aliphatic tails which partition into the lipid bilayer, leaving the fluorophore on the external leaflet. FRET can occur between lipophilic donors and acceptors within a lipid mixture if their spatial separation is typically < 8 nm. Absorption and normalized fluorescence emission spectra of membrane-bound (b) DiO (blue), DiI (orange), DiD (red) and (c) DiA (blue) and 4-Di-10-ASP (cyan).

A wide range of organic dyes also exist for the non-covalent labelling of DNA molecules. These can be broadly classified into three major classes: groove binders, intercalators and cationic electrostatic/allosteric binders that bind to the negatively-charged phosphate backbone via attractive ionic interactions (**Figure 4a**)[89]. In the latter case, positive charges on the probe arise from the existence of an exocyclic ammonium or endocyclic pyridinium moiety. The intercalators, which can be cationic or neutral, bind to the DNA by inserting aromatic groups between adjacent base pairs, with representative examples including ellipticine, proflavine, acridine orange, methylene blue, ethidium bromide, thiazole orange, the SYTOX derivatives and YOYO-1. In the case of ellipticine molecular dynamics simulations indicate rapid intercalation timescales (~0.8 ns) (**Figure 4a**) and in nearly all cases, variations in the absorption and emission properties upon binding, has enabled a multitude of imaging-based experiments.

Visualization of single double-stranded DNA molecules undergoing conformational changes was initially achieved via fluorescence from 4',6-diamidino-2-phenylindole (DAPI) upon interaction with adenine-thymine rich regions[90]. In such examples, we note that single intercalators and not visualized per se, but rather the nucleic acids are observed via multiple fluorescing labels. However, relatively low binding affinities and poor photophysical properties motivated the development of a new class of dyes that undergo quantum yield enhancements upon DNA binding. The most widely used of these probes for single-molecule research are YOYO-1 and SYTOX Orange (SO).

YOYO-1 (**Figure 4b**) is a cyanine derivative with peak absorption and emission at 491 nm and 509 nm, respectively (**Figure 4c**), and binds to double stranded DNA with high affinity (k_D ~ 5-50 nM)[91]. Fluorescence enhancements of ~1000-fold occurs upon binding, leading to the high signal-to-noise ratios necessary for nucleic acid detection. YOYO-1 has, for example, helped researchers to identify conformational changes in single DNA molecules during replication[92], and has facilitated quantification of base-pair orientations via polarization microscopy[93].

SO, also a cyanine derivative with peak absorption at 547 nm and emission at 570 nm (**Figure 4c**) intercalates into double stranded DNA as a monomer[94] and undergoes substantially greater emission intensity enhancements upon binding (> 1000-fold). While the chemical structure of SO is proprietary, the reported dissociation constant of ~10 nM is of similar magnitude to that observed by YOYO-1. The kinetic binding rates are, however, an order of magnitude faster, enabling labelling to be achieved almost immediately[95]. As shown in **Figure 4d**, the most versatile application involving intercalators has been the DNA curtains technique[96], where single surface-tethered DNA molecules are stretched under flow containing nM concentrations of intercalator, and visualized by techniques such as total internal reflection fluorescence microscopy (TIRFM). The method allows for the parallel imaging of hundreds of aligned molecules and presents a robust experimental platform from which to investigate a multitude of protein- and enzyme-DNA interactions with millisecond timescale resolution.

The time constant of DNA intercalation depends on the number of intercalating moieties and the overall timescale required to reach equilibrium. The process can involve the insertion of a single moiety per probe, as is the case for ellipticine (**Figure 4a**), two moieties per probe, such as for YOYO-1 (**Figure 4b**) or multi-intercalating sub-units. The timescale for reaching the final equilibrium state ranges over six orders of magnitude, though we note this is likely contingent upon the DNA template used, its structural conformation, the free energy landscape, and the accessibility of intercalation sites[97]. The association rates and mechanisms of intercalation vary from probe-to-probe but in general, the association rates of traditional mono- and bi-intercalators, are several orders of magnitude faster than the association rates of unconventional groove binders. The mono-intercalator ethidium bromide displays association kinetics of only a few milliseconds in the ensemble, and bis-intercalators, including YOYO-1 intercalate with a typical time constant of a few seconds. On the other hand, unconventional binders, including actinomycin D, generally display slow association kinetics on the order of several thousand seconds, though destabilization of double stranded DNA by force has been shown to exponentially facilitate the on rates[98]. Importantly, fast association rates are characteristic for common mono- and bis- cyanine-based intercalators and therefore one can suppose that structurally similar derivatives will display similar traits. The fast association rates achievable using mono- and bis-intercalators relative to the nominal timescale of typical DNA curtains experiments (~10-100 s) thus provide the basis for examining single nucleic acids in vitro. YOYO-1 has also been employed for high precision microscopy of single DNA molecules by utlising its stochastic, reversible photolinking to generate super-resolved localized data of labelled DNA[99].

Despite indications that YOYO-1 and SO may subtly alter the mechanical and structural properties of DNA upon binding[100, 101], recent work has established that the persistence length and rigidity remain unaffected[102]. In addition, the binding affinities are governed by a strongly tension-dependent but tuneable dissociation rate, and optimization of this parameter can reduce the effect of the intercalators on strand separation and enzymatic function[103].

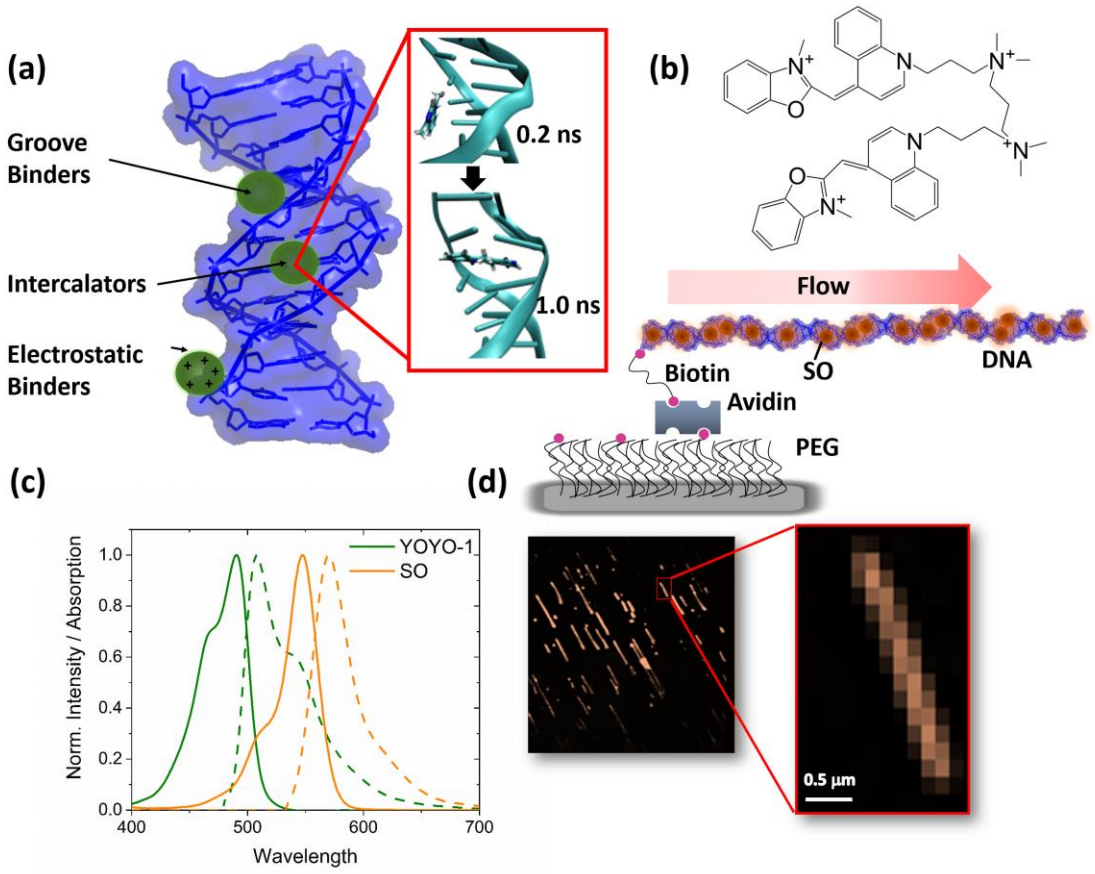

Figure 4. Commonly used intercalators for visualization of single nucleic acids. (a) Schematic illustration of different DNA binders. The DNA backbone (PDB ID: 1BNA) and base pairs are shown in blue. Inset: ellipticine (represented by a ball and stick model) intercalates into the DNA bases (represented as rods) over ~0.8 ns as suggested via targeted molecular dynamics simulations. (b) Chemical structure of YOYO-1. (c) Absorption (solid lines) and fluorescence emission spectra (dashed lines) of YOYO-1 (green) and SYTOX Orange (orange). (d) Representative TIRFM images (lower panels) of single λ-DNA molecules immobilized onto a glass coverslip coated in polyethylene glycol (PEG) via biotin-streptavidin interactions in the presence of 1 nM SYTOX Orange under 20 µL/min flow conditions (top panel).

To complement the use of organic dyes for direct and indirect biomolecular labelling, several organic dyes have been developed to sense the biomolecular environment. These include sensors which quantify the presence of metal ions and report the solution pH. Currently, there is no single dye that permits measurement of all environmental parameters directly within a single sample, but combinations of fluorescent organic dyes hold promise in this regard. Generally, these sensors are designed to measure free hydrated ions, whilst not engaging in competitive exchange[104]. The majority of the probes undergo quenching between the metal binding domain and the fluorophore via photoinduced electron transfer (PET) in the absence of the ions, and undergo a fluorescence enhancement during binding due to PET-disruption. Derivatives of fluorescein, including the Zinpyr (ZP) family of dyes have been employed as sensors of Zn^{2+} in live cells. ZP1, which contains a di-2-picolylamine Zn^{2+} chelator and a dichlorofluorescein emitter[105] is an established sensor of metalloneurochemistry[106], but next-generation probes, such as ZP2, ZP3 and ZP4 have since offered a 6-fold increase in dynamic range, lower pKa values, simpler synthesis procedures and enhanced signal-to-noise ratios. ZP1 derivatives, including ZnAF-1F and ZNAF-2F, in which the fluorine at the orthoposition of the phenolic hydroxyl group has been substituted, now offer a 69- and 60-fold fluorescence enhancement, respectively, when fully bound to Zn^{2+}. However, the quantum yields of both

probes in the absence of Zn^{2+} are relatively low (~0.006), rendering their single-molecule detection challenging[107].

A number of Zn^{2+} probes have also been designed based on the structures of existing Ca^{2+} sensors, and of these, FluoZin-3 is one of the most widely used[108]. Here, an acetate group on the Ca^{2+} chelator has reduced affinity for Ca^{2+}, while offering a 200-fold fluorescence enhancement in the presence of Zn^{2+} (k_D ~15 nM). A growing number of similar small molecule sensors have been developed to measure vesicular Zn^{2+} pools, including Zinquin[109], ZincBy-1[110], SpiroZin1[111], and SpiroZin2[112], though differences in emission stability and non-specific localization vary from probe-to-probe and must be taken into consideration[113].

In a similar way, the development of Ca^{2+} indicators[114] have led to important insights into signalling pathways[115]. Ca^{2+} sensors typically undergo either a fluorescent enhancement or decrease to reflect changes in the local Ca^{2+} concentration, though it is worth noting that indicator concentration, cytosolic location and pH may also contribute. These indicators are generally divided into single-colour or ratiometric probes based on their response to Ca^{2+}[116, 117]. Single-colour probes, such as Fluo-4, displays a >100-fold increase in fluorescence intensity at 506 nm, whereas ratiometric indicators exhibit shifts in excitation and/or emission wavelengths upon binding. Consequently, single-colour probes are generally used for qualitative estimates of Ca^{2+} levels. Recently, the Cal-520 probe, which undergoes a two-fold increase in brightness when fully bound to Ca^{2+}, has been used probe protein- and surfactant-induced permeabilization in lipid vesicles, and offers a promising alternative[21, 118, 119]. Conversely, when Ca^{2+} binds to ratiometric indicators such as Indo-1 and Fura-2, emission enhancements at shorter wavelengths concurrent with emission reductions at longer wavelengths typically occur, facilitating quantitative estimates of Ca^{2+} molarity. In the case of Fura-2, the requirement to perform alternating excitation at 340/380 nm can hinder data acquisition, though it has a higher dynamic range when compared with Indo-1.

It comes as no surprise that the design, synthesis and characterization of a wide variety of organic dyes, using an assortment of fluorogenic units have preceded a range of single-molecule applications. Yet while the rhodamine and fluorescein derivatives generally exhibit high quantum yields (> 0.9) and good photostability, their biological applications have been limited because their absorption and emission range extend only up to 600 nm. For single-molecule detection in living cells, autofluorescence is substantially reduced at wavelengths > 600 nm, and thus red- and near-infrared wavelengths offer an overall improvement to the signal-to-noise ratio. Similarly, although cyanine dervitavies have been extensively used, they are only moderately photostable. In this regard, rylene dyes formed via the linkage of naphthalene units in peri-positions, are known to have high quantum yields, some even as high as 0.8-0.9, are generally much more photostable than commercially available cyanines (typically by a factor of ~100), with uncharged species showing particular promise in this area, and are available with emission > 600 nm[120]. Historically, a major limitation of rylene dyes for biological applications was their relatively poor solubility, but recently, the introduction of ioinic sulfonyl, pyridoxy, polyethylene glycol and peri-guanidine side groups have helped alleviate this issue and have facilitated a wide-range of single-molecule and live-cell experiments[120-122]. Most can also be modified with functional groups for biomolecular labelling. Of particular note, the development of perylene diimides have shown particular promise for imaging membranes, biosensing in vitro, detecting antibodies, monitoring cellular uptake, and detecting gene/drug delivery in living cells[123]. While solubility has vastly improved, minimizing undesirable self-aggregation properties of rylene dyes is still an area of concern, though clearly exciting prospects lie ahead for this class of organic probe.

In addition to the rylene dyes, water-soluble dyes containing diketopyrrolopyrroles (DPPs) have also offered attractive properties to the single-molecule community because of their excellent photostability and high quantum yields (0.4 - 0.9). The general DPP structure is synthesized by the reaction of aromatic nitrile with dialkyl succinate to produce a planar structure with strong intramolecular hydrogen bonding and π-π stacking between adjacent molecules, both of which are key to its chemical stability. Of particular note is the presence of a bicylclic lactam chromophoric unit containing three different functional groups (-C=C- double bonds, carbonyl and amine (NH) groups) that may be used as building blocks for further synthetic modification and derivitization, and as a platform for a vast array of functionalization possibilities. The biological applications, especially in living cells, have however been limited because most DPP derivatives absorb in the range 435-510 nm and emit < 600 nm. That said, with moderately high extinction coefficients (~25,000 $M^{-1}cm^{-1}$) of solution and membrane-bound forms, considerable effort has been dedicated to their single-molecule application. For example, recent work involving structurally rigid L-shaped isoindoledione, produced via DPP synthesis, has enabled solvent-sensitive emission up to ~630 nm with large Stokes shifts to be achieved while minimizing autofluorescence[124]. In the same work, an N-alkylated isoindoledione containing a benzofuryl substituent was found to stain cell membranes exclusively, though a substantial reduction in quantum yield by comparison was noted. The use of DPP-based probes has also emerged as promising with respect to molecular imaging, and several studies have explored the two-photon absorption properties of DPP-conjugated dyes, demonstrating their potential utility for deep imaging. In this regard we refer the reader to an extensive review in this area[125]. The application of ratiometric DPP containing probes have also demonstrated specificity towards esterase in cells, even in the presence of other analytes[126].

Over the years, organic dyes have found vast utility in the context of single-molecule detection, imaging and quantification. However, for many applications, especially those involving live-cell imaging, they have taken somewhat of a backseat, owing in-part to the development of genetically encoded fluorescent proteins.

2.2 Fluorescent Proteins

The purification of the green fluorescent protein (GFP) from *Aequorea victoria* jellyfish[127] revolutionized the single-molecule field and led to methods of expressing translationally fused fluorescent proteins as labels of proteins of interest via genetic engineering, bypassing the need for any form of chemical attachment (**Figure 5a, b**)[128-130]. Unlike quantum dots and organic dyes, which require appropriately designed conjugation schemes, fluorescent proteins offer a valuable alternative for *in cellulo* and *in vivo* imaging. A second appealing characteristic rests in their ability to confer high cellular and sub-cellular specificity using promoters, enabling these probes to report from specific, often otherwise inaccessible regions. Additionally, fluorescent proteins are easily inserted into live cells by transfection or virus infection and can be upheld for timescales far surpassing 24 hours prior to excretion[131]. Fluorescent proteins have thus been applied extensively – for example in live cell FRET biosensing experiments[132], as both donors and acceptors, in fluorescence lifetime imaging (FLIM) for the detection of protein-protein interactions [133], interrogating the dynamic interplay between proteins and lipids[134] and to count the number of subunits in functional molecular machines[99].

Among the most widely used FRET sensors is the blue-yellow mTurquoise2 (donor) and sEYFP (acceptor) pair which provides a Förster radius of 5.9 nm and ~2-8 nm

sensitivity[133]. Derivatives of sEYFP also exist (including mVenus, mCitrine and YPet), and each has been tailored to accommodate minor pH switching[135-137]. A major limitation of long-term FRET imaging, however, is their relatively poor photostability. The emission signal often dissipates rapidly over time, thereby affecting the ratio of donor to acceptor emission intensities and necessitating corrections for photobleaching. It follows that fluorescent proteins for FRET-based applications should be chosen based on high brightness, long-term photostability and insensitivity to pH fluctuations. Unfortunately, engineering fluorescent proteins with all desired properties remains a major experimental challenge, though progress has been made with the development of mClover3 and mRuby3. In such examples, oxygen access to the chromophores is limited[136, 138]. Pairs such as mClover3-mRuby3 or similarly, mNeongreen-mRuby3 therefore hold promise for live-cell FRET imaging in the future. On the other hand, EYFP and mCitrine are strongly pH-sensitive and therefore have potential for detecting activities such as protein function, metabolic reactions and autophagy, where pH regulation is critical[139].

Green-red FRET pairs, such as the EGFP-mCherry (**Figure 5b,c**) and GFP-mRuby2 combination overcome some of the limitations of blue-yellow pairs. For instance, excitation in the green generally reduces autofluorescence, the proteins are less phototoxic, they exhibit greater spectral separation and they have extended distance sensitivity [140-142]. Furthermore, unlike other fluorescent proteins, mCherry emission is only rarely interrupted by photoblinking. FRET pairs with spectra in the far-red, such as the mPlum-IFP1.4 duo[143], have the additionaladvantages of further reducing autofluorescence and offer the potential for deep-tissue imaging, though further developments in this area is required to improve overall brightness.

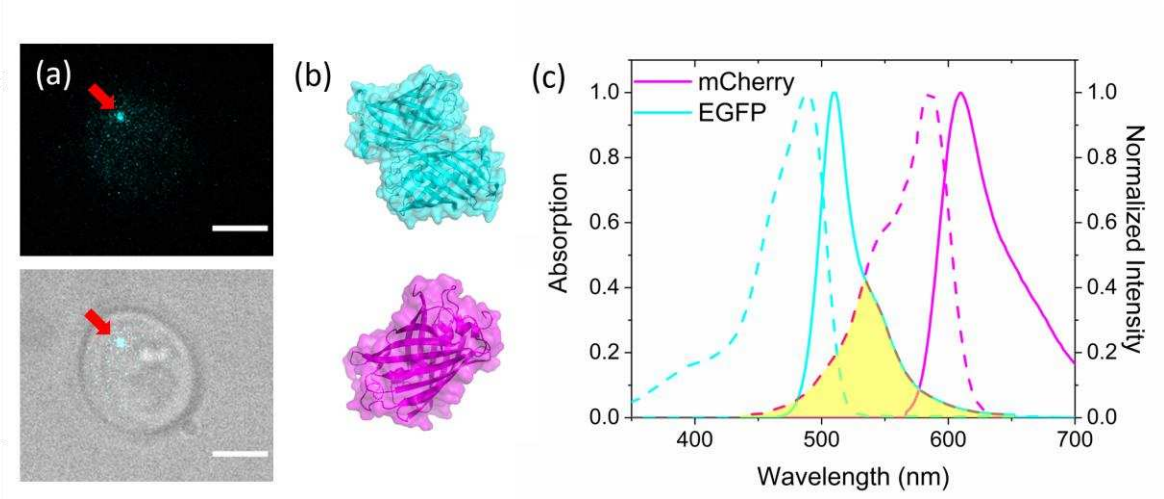

Figure 5. Single-molecule imaging of fluorescent proteins. (a) Saccharomyces cerevisiae under glucose depletion. Here, the Mig1 repressor is fluorescently labelled with GFP (cyan). Representative fluorescence image obtained via Slimfield microscopy[144] of a single Mig1-GFP molecule (top panel) enables its spatial position within the cell to be evaluated when overlaid and compared against the corresponding brightfield image. (b) Crystal structures of GFP (top panel, PDB ID: 1GFL) and mCherry (bottom panel, PDB ID: 2H5Q) showing locations of the alpha helices, beta strands and coiled-coiled regions. (c) Absorption (dashed) and fluorescence emission (solid) spectra of EGFP and mCherry demonstrating the spectral overlap (yellow shaded region) necessary for compatibility with single-molecule FRET imaging.

Although blue, green, yellow and red fluorescent proteins have been extensively used, their complicated photophysics, coupled with photostability issues, mean that their application in

single-molecule experiments is still challenging. To help bridge this gap, photoactivatable and photoswitchable fluorescent proteins have been engineered to aid with diffusion studies and to understanding pathways. While the former are induced to switch from a low-emissive dark state to an emissive bright state, the latter are stimulated to emit at shifted wavelengths[145]. Among these derivatives, the photoactivatable variant of GFP, avGFP, exhibits an excitation spectrum with two distinct peaks (396 nm and 476 nm) corresponding to protonated and deprotonated chromophores. Upon UV excitation, the ratio of these peaks changes in favour of the deprotonated form[146]. The photoactivatable and switchable properties of such fluorescent proteins allow the labelled biomolecule to be tracked without the need for continuous visualization, which goes some way to overcoming the issue of low photostability.

It comes as no surprise that many challenges remain in this area, not least of which is the need to engineer fluorescent proteins with higher quantum yields. One potential strategy to achieve this is to develop a suite of fluorescent proteins with improved maturation and folding attributes. Furthermore, one should be aware that self-assembling fluorescent proteins, caused by hydrophobic mutations can interfere with FRET-based distance conversions, though modifications of peptide linkers between fluorescent proteins and the sensing region could be a potential strategy to overcome this[147]. The relatively large size of fluorescent proteins mean that they can also interfere with, for example, kinase motion, though some fluorescent proteins bypass this by reporting on nucleo-cytoplasmic shuttling readouts[148].

2.3 Quantum Dots

Quantum dots (QDs) are nanoparticles composed of periodic groups of III-V, II-VI or IV-VI semiconductor materials such as CdS, CdSe, CdTe, ZnS, ZnSe and InP with tuneable physical dimensions as well as optoelectronic properties which are not available from isolated molecules or bulk solids. They exhibit discrete energy levels and their bandgap can be precisely modulated by varying their size. Their high emission intensities, large Stokes shift, narrow emission and broad absorption spectra, large molar extinction coefficients, high quantum yields, strong resistance to photobleaching and long fluorescence lifetimes[149-152] have made them particularly attractive across the single-molecule community as *in vitro* and *in vivo* biosensors[153], and their production has also led to substantial contributions towards the development of super-resolution imaging and single-particle tracking[154] techniques. Furthermore, their electronic features are enabling the development of QD-based electrochemical[155] and electroluminescent biosensing either as a catalyst or light-emitter, and recent developments have even seen them used as single particle drug delivery vehicles[156].

QDs are typically prepared using organometallic chemistry methods[157] to yield emission wavelengths spanning across the UV, visible and infrared. For biological applications, it is critical to render the QD soluble through surface-passivation, with the ideal water-soluble ligand (i) enhancing QD stability, (ii) maintaining resistance of the QD to photobleaching and degradation, (iii) containing functional groups for bio-conjugation and (iv) minimizing the particle size. While the physical and optical properties of QDs have been extensively studied for single-molecule applications such as multiplexed imaging[158] *in vivo* bio-detection[159] and FRET [160], CdTe and CdSe derivatives have attracted particular attention owing to their versatility.

CdTe is a II-VI semiconductor with a bandgap energy of ~1.5 eV at 300 K[161], corresponding to infrared emission, but as its size is reduced to the order of several nanometres via the quantum confinement of charge carriers, the fluorescence emission wavelength peak shifts through the visible range (500-750 nm). As the density of states near the conduction and valence bands reduces < 12 nm, discrete excitonic states form. Consequently, the bandgap increases, resulting in a peak shift of the spectrum[162] (**Figure 6**). In a similar way, the bandgap of CdSe QDs increases from 1.9 eV to 2.8 eV as the size decreases from 7 nm to 2 nm, enabling tailored emission in the range 450-650 nm[162]. We note that on comparison to core-type CdTe QDs, core shell CdSe/ZnS particles exhibit narrower emission features (**Figure 6**), though the precise range over which emission occurs and the spectral properties ultimately depend on the materials used, surface coatings and particle size. Though CdTe and CdSe are among the most widely used of all QDs, the implications of the Cd/Te and Cd/Se molar ratios on optical properties such as emission intensity, quantum yield and lifetime is a relatively new area that demands further exploration[163, 164]. Nevertheless, their high quantum yields (20-80 %) place them among the brightest of all available probes[165]. Their extinction coefficients associated with the first excitonic absorption peak, though strongly size-dependent, are relatively large (ε = 1 - 8 x 10^5 $M^{-1}cm^{-1}$)[166] and their two-photon absorption cross sections are orders of magnitude larger than those associated with organic dyes[162]. We note that the extinction coefficients at the first exciton peak are much lower than those at shorter wavelengths, in contrast to organic dyes which have their largest extinction coefficient at the peak of their absorption spectrum. Coupled with their broad excitation spectra which increase towards the UV, relatively long lifetimes (> 10 ns) and resistance to chemical degradation, CdTe and CdSe QDs are excellent candidates for tracking time-dependent dynamic processes[154], biomedical imaging including *in vivo* tumour detection[167, 168], deep tissue imaging[169], environmental sensing[170, 171] and antibody detection[172].

Core-type QDs such as CdTe and CdSe do however suffer from lower quantum yields and photostability[173] though this can be improved by passivation of the surface with semiconductors such as CdS or ZnS. Some common examples of these so-called core-shell QDs include CdS on CdSe and ZnS on CdSe, the latter containing a larger fraction of brighter particles relative to the core-type case as a result of increased single-particle quantum yields[174]. The application of such QDs in single-molecule imaging has been mainly directed towards mammalian cells, though there is an increasing tendency to apply them for intracellular tracking, diagnostics, *in vivo* imaging and therapeutic delivery[175] and, for electrochemiluminescene assays where femtomolar detection of single particles is now possible[176, 177]. For example, the single-particle tracking of QD-conjugated membrane receptors[178] and proteins[179, 180] in living cells has enabled their diffusion characteristics in response to environmental stimuli to be accessed for long timescales (> 20 min) and temporal resolutions (< 1 ms[181]) surpassing those conventionally accessible using organic dyes. Further QD tracking applications have included their use as tumour-targeting drug delivery vehicles[182] and as encapsulated cargo within synaptic vesicles[183]. QDs have also found utility as effective single-particle FRET acceptors, though their long fluorescence lifetimes dictate the need for donors with comparably long lifetimes, such as lanthanide dyes, as opposed to organic dyes, for detectable FRET[184]. It follows that QD-based single-particle detection offers multifunctional and attractive opportunities for probing and manipulating biological systems, both *in vitro* and *in vivo*, but great care must be taken during their synthesis and integration with biological molecules to avoid perturbing function.

To harness the attractive optical properties of QDs, it would be ideal to minimize their size for biomolecular-labelling. Being comparably large, with often insoluble properties and being incapable of precise valency controlled labelling, they rely heavily on being passivated with organic ligands. While the ligands should improve QD solubility, they must

also provide the QD surface with a chemical platform from which to enable effective and efficient biomolecular conjugation[185-187]. CdTe QDs, for instance, are typically capped with mercaptopropionic acid or mercaptosuccinic acid terminated with –COOH for these reasons[188]. Recently, QDs wrapped in functionalized oligonucleotides have shown promise in the context of single particle tracking[189, 190], ligands covalently coupled to polyethylene glycols have helped to minimize nonspecific binding[191, 192], and water-dispersible QDs comprising hydrophobic QDs and zwitterionic moieties have realized liposomal-like structures that preserve optical and colloidal stability[193]. Amphiphilic polymers have also been used to improve bioconjugation[194], and although challenges still exist, strategies for producing monovalent QDs have been reported[194, 195]. We direct the reader to comprehensive reviews in these areas[192, 194, 196, 197]. Despite such advances, the QD size, solubility and valency of labelling are still significant hurdles that must be overcome when QDs are employed as single-particle sensors.

An interesting property of quantum dots is their fluorescent intermittency, whereby the fluorescence intensity from a single QD fluctuates between highly emissive 'on' states and non-emissive 'dark' states (**Figure 6**). While the root cause of photoblinking is still debated, evidence points towards a mechanism in which electron transfer to trap states in the QD or surrounding matrix leads to photoinduced charging[198, 199]. QD photoblinking provides a simple way of achieving super-resolution localization via conventional fluorescence microscopy[200] and blinking rates may be modulated in the presence of ions, offering environmental sensitivity[170, 201, 202]. Taken together, understanding, suppressing and manipulating the blinking characteristics of QDs are important lines of single-particle research.

Importantly, not all QDs are identical, and they cannot be considered as a uniform group. QD toxicity, for example, is closely linked to the intrinsic properties of the quantum dot, including material, shell type, ligand, surface chemistry, and size[203]. A number of assays have been employed over the years to evaluate the influence of QDs on cellular organelles, protein expression, and clearance mechanisms, and in some cases QD modifications have been made to mitigate against the effects, but it is important to note that while some examples of QD have demonstrable influence on biological function, others, have minimal influence[203-206]. While it is outwith the scope of this review to provide an exhaustive list of QD flavours and their reported toxicities, care must be taken to minimize or reduce toxicity, either through careful choice of QD or QD modification, and this is especially true in the context of live-cell applications[201].

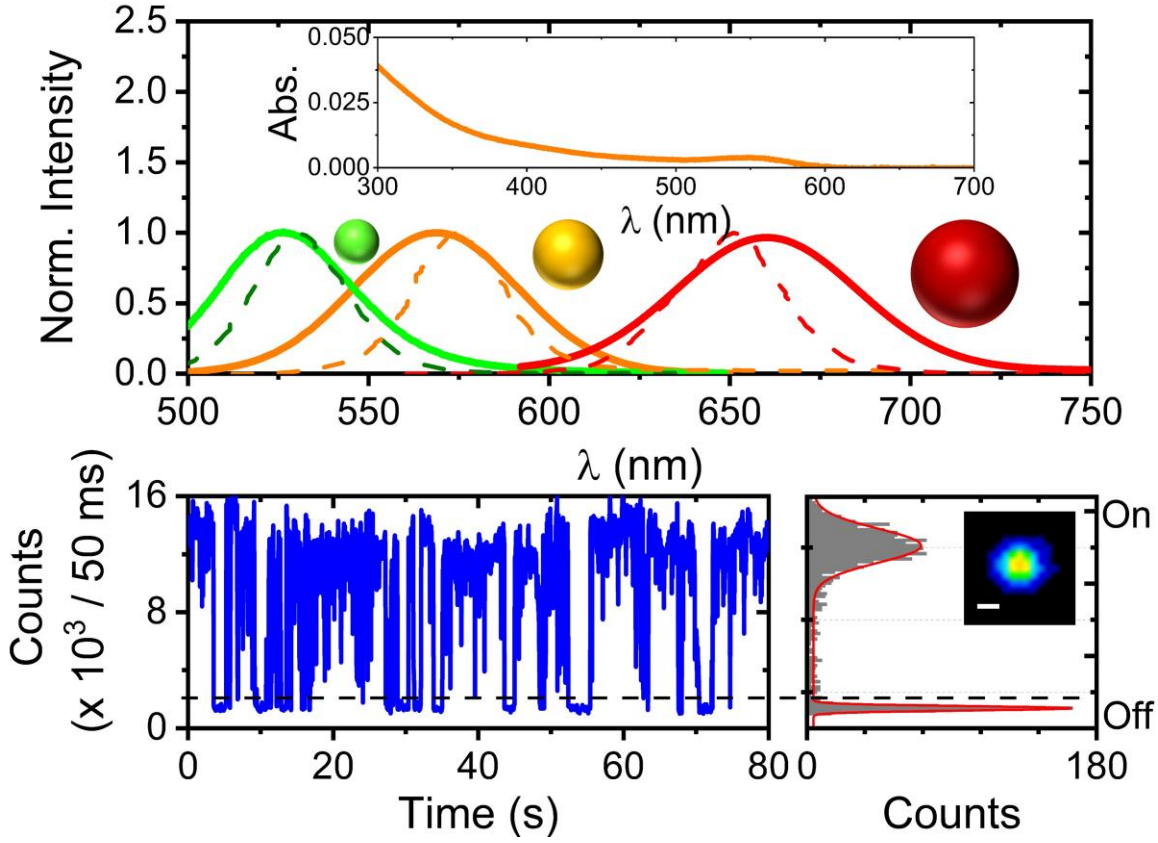

Figure 6. Fluorescence emission of single quantum dots. Top panel: Size-dependent emission spectra associated with CdTe and CdSe/ZnS quantum dots. Shown are representative emission spectra for core-type CdTe-530 (solid green) (inset: absorption spectra), -580 (solid orange) and -680 (solid red) and CdSe/ZnS-530 (dashed green), -580 (dashed orange) and -650 (dashed red). Lower panel: Representative single particle fluorescence trajectory (left panel) and corresponding intensity histogram (right panel) indicating photoblinking from highly emissive 'on' states to non-emissive 'off' states obtained from TIRFM imaging of a single CdTe 580 QD (inset, scale bar = 500 nm). The dashed line corresponds to a threshold intensity level of 6 standard deviations above background used for differentiating between on and off states.

2.4 Fluorescent Nanodiamonds

Fluorescent nanodiamonds (FNDs) are now emerging as promising biomarkers for single-molecule applications. While FNDs can be easily detected by conventional fluorescence microscopy, unlike QDs and organic dyes, their existence inside the cell does not induce cell death[207]. FNDs have been reported to be over an order of magnitude brighter and more photostable than conventional organic dyes[208], and many display spectral shifts in response to changes in magnetic fields, electric fields and temperature gradients, making them useful nanosensors for high-resolution imaging[209]. The tuneable emission properties arise from the doping of nanodiamonds with defects such as nitrogen-, europium- and silicon-vacancies (**Figure 7a**). These behave like isolated atoms or molecules in a host matrix, with emission stemming from these locations as opposed to the bulk material [210-215] (**Figure 7b**). Fluorescence arising from nitrogen-vacancy doped FNDs are photostable, even after months of continuous excitation[216]. While they are also known for their biological inertness, successful FND-labelling of proteins[217, 218] and DNA[219] has been achieved since their surface can be terminated with oxygen or hydrogen.

Of all FNDs, those which are nitrogen-vacancy doped have shown particular promise for single-molecule applications, though it is worth noting that only a fraction of elements in the periodic table have been incorporated as defects. Not only are they now routinely used for long-term particle tracking and localization in live cells,[220-222] owing to their excellent photostability, they have also been used to sense magnetic fields through spectral shifts in their fluorescence emission, revealing FND orientation in the process[222]. Their application has also extended to FRET-based sensing, where nitrogen-vacancy doped FNDs have acted as donors for black hole quenching dyes such as DY781[223], or as GFP acceptors for observing rotational motion in the F_0F_1 ATP synthase[220].

For future single-molecule applications where small-sized FNDs are required, it may be possible to prepare them with specific numbers of defects per nanodiamond, while maintaining photostability, and natural extensions are far reaching.

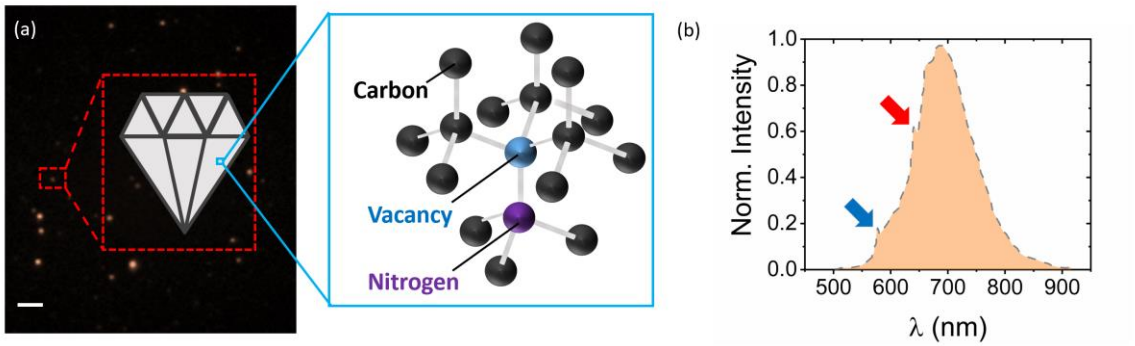

Figure 7. Fluorescence emission of single nanodiamonds. (a) Widefield TIRF image of single nanodiamonds (scale bar = 1 μm) and inset, structure of the nitrogen-vacancy defect. (b) Normalized fluorescence emission spectra obtained from 100 nm-sized nitrogen-vacancy center fluorescent nanodiamonds at a concentration of 1 mg/mL in ultra-pure water (λ_{ex} = 532 nm). The emission spectrum displays zero phonon lines at 638 nm (red arrow) and 575 nm (blue arrow) corresponding to the presence of negatively charged and neutral defects, respectively.

3. Conjugation strategies for single-molecule probes.

Coupling the probe of interest can be achieved by direct and indirect labelling methods, but challenges of controlling specificity and defining stoichiometry must be overcome for successful conjugation. In this section we discuss various labelling methods, highlighting the advantages and limitations of each approach, such that careful selection of the best method can be chosen.

3.1 Direct labelling with organic fluorophores

Techniques for chemically attaching organic fluorophores to target biomolecules have been critical for single-molecule imaging applications. Of all the techniques available, the site-specific covalent labelling of proteins with organic dyes has enabled the development of several single-molecule assays[224]. Direct chemical attachment of purified proteins involves targeting the amino acid cysteine and amine groups (**Figure 8a**). In cysteine, a free sulfhydryl group can be rapidly cross-linked to an organic dye chemically engineered to contain a thiol-reactive agent such as maleimide, offering a highly specific and rapid labelling reaction under moderate conditions[49]. Surface-accessible cysteines are

particularly appealing for labelling because they are found in relatively low abundance. If necessary, they can also be introduced into an amino acid sequence using site-directed mutagenesis[225], though we again emphasise that care must be taken not to perturb the overall function of the target biomolecule[226, 227]. It may also be possible to selectively label a cysteine by inducing conformational changes to improve site accessibility[228] or by manipulating the reversible protection of cysteines using metal ions[229].

Under all conditions, the target protein must be maintained in a reduced form (using for example, dithiothreitol (DTT) or tris[2-carboxyethyl]phosphine (TCEP)) prior to the labelling reaction in order to prevent the formation of disulphide bridges and the inactivation of cysteines. Immediately prior to labelling, the reducing agents should be removed to prevent reoxidation and the thiol groups competing with the target thiols on the target biomolecule. Furthermore, the efficient removal of unreacted molecules prior to single-molecule imaging is key to avoid the presence of free dye within the measurement.

In a similar way, amine-reactive conjugates, such as N-hydroxysuccinimide (NHS) ester or isothiocyanates can be used for the specific labelling of lysine or N-terminal amines (**Figure 8b**)[230, 231]. However, unlike cysteines, lysines are found in relative abundance and can therefore be problematic when the aim is to directly attach a single probe.

Site-specific conjugation via encoded unnatural amino acids (UAAs) and highly-specific biorthogonal reactions also provides a useful way of directly conjugating probes to a protein structure, and in general, this strategy overcomes some of the problems associated with cysteine labelling (**Figure 8c**)[232]. UAAs generally containing ketone, azide, alkyne or tetrazine groups can be encoded into the protein structure via modification of the cDNA sequence in response to a unique amber stop codon. These groups can then be coupled to functionalized dyes via high-yield click chemistry procedures[233, 234]. In general, if the protein only contains1-2 regular amino acids, then these can be replaced with the UAA during protein expression[235-237]. Nonsense codons which encode the UAA selenocysteine (SeC) into the protein structure are particularly attractive due to their ease-of-conjugation towards organic dyes containing maleimide or α-haloketones. By far the most common UAAs incorporated into protein structure are designed to undergo alkyne-azide click chemistry and useful examples include the labelling of azide-containing UAAs incorporated into the protein structure with Alexa Fluor 488-Alkyne[238]. Here the chemical reaction uses copper as a catalyst and results in a highly selective and strong covalent bond formed between azide and alkyne chemical groups to form stable 1,2,3-triazoles. The UAA p-acetylphenylalanine, for example, can be incorporated into a protein structure in response to the TAG stop codon, and this reacts well with organic dyes containing hydroxylamine groups, though the reaction must be carried out at low pH[239]. Propargyl lysine is an alternative option used to couple azide-modified fluorophores to the structure via copper catalysed alkyne-azide cycloaddition (**Figure 8c**)[240]. Efficient incorporation of UAAs into protein structures has enabled a variety of applications, including but not limited to single-molecule FRET studies on the T4 lysozyme[241], intracellular DNA-PAINT[242], and the super-resolution imaging of outer-membrane proteins in E. coli.[243]. To extend their utility further, unnatural fluorescent amino acids, such as Lys(BODIPYFL)[244], 4-cyanotryptophan[245] and dansyl alanine[246] have emerged for single-molecule studies of ion-channels and protein folding, and this is an exciting area that warrants further investigation.

For the site specific labelling of DNA and RNA molecules, short nucleic acid oligo inserts can be used. In this case a nucleic acid sequence can be cut at specific locations by restriction endonucleases to enable short sequences of nucleic acids complementary to a specific oligo sequence to be inserted at that location. Incubation with the oligo will then

result in binding to the complementary sequence[247-249]. This is particularly useful since oligos can be modified to include a variety of chemical groups, including biotin, azide and alkynes to enable conjugation. Recently, bright and photostable fluorescent RNAs have also facilitated cellular RNA tracking experiments within living systems[250].

In most cases, and irrespective of the length of the conjugation linker, the fluorophore can conformationally diffuse within an accessible volume around the attachment site (**Figure 8d**)[32]. In the case of FRET-based measurements, this can lead to uncertainties in accurate distance determination and hinder experiments where short distance ranges between the attachment points are required due to dye-dye interactions[251]. It is therefore of utmost importance that in such applications, the positional distribution of the dye is assessed via geometric accessible volume simulations[31, 252], provided that the local structure of the biomolecule is known, in order to obtain accurate quantitative details[33].

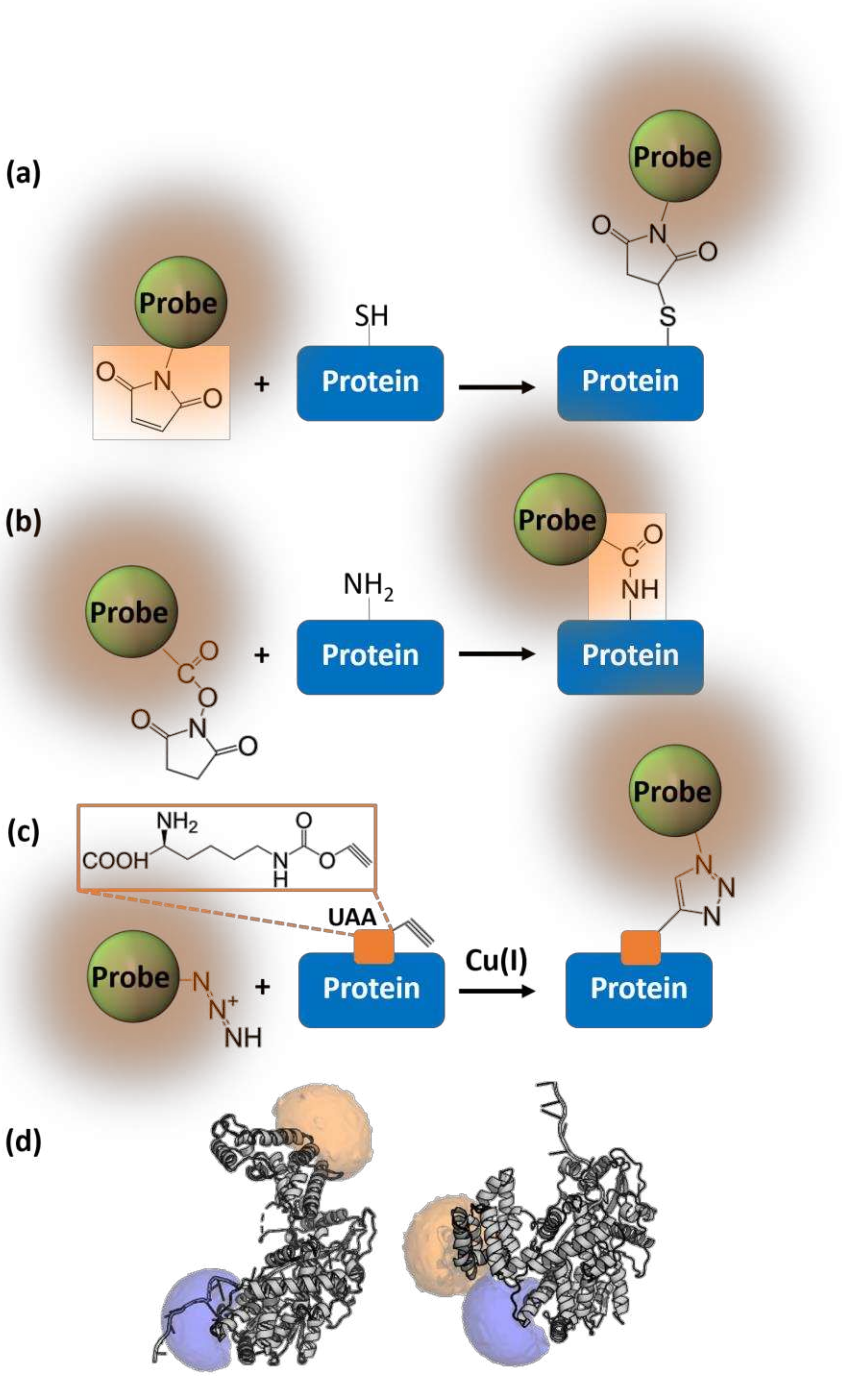

Figure 8. Comparison of commonly used protein labelling methods. Schematic illustrations of labelling reactions involving (a) maleimide functionalized probe and surface accessible cysteine, (b) succinimidyl-ester functionalized probe and amine group and (c) azide functionalized probe and alkyne group on a surface accessible unnatural amino acid. Inset: chemical structure of the UAA propargyl lysine. (d) Accessible volumes of Alexa Fluor 546 (blue) and Alexa Fluor 647 (orange) tagged to Cys97 and Cys473 on the Rep helicase are illustrated as semi-transparent surfaces in the open (left) and closed (right) conformations[253].

3.2 Protein Tags

Direct protein labelling is often limited by low yield, high levels of impurities or situations where the direct attachment of large fluorophores alters the activity of the biomolecule[254, 255]. The use of protein tags, such as the polyhistidine (His) tag (**Figure 9a,b**) have thus emerged as powerful tools for overcoming such issues. Here the low molecular weight tag is attached to recombinantly expressed proteins, enabling downstream labelling to anti-His functionalized probes to be attached with high specificity[256]. For live cell approaches, however, additional methods of labelling are required. Using a strategy complementary to immunostaining or antibody-labelling, a widely adopted strategy to perform site-specific fluorescent labelling a protein of interest is to express it fused with a monovalent tag using a single genetic construct which enables the downstream attachment of a functionalized fluorophore. Among these include SNAP- (**Figure 9c**) and CLIP-tags which are derivatives of the 20 kDa DNA repair protein O^6-alkylguanine-DNA alkyltransferase[255]. The tags are specifically designed to irreversibly attach to O^6-benzylguanine functionalized dyes via a stable thioether bond using a reactive cysteine in the tag[257]. Protein tags have thus found applicability in the detection and quantitation of labelled proteins via conventional biochemical methods such as in-gel fluorescence scanning of SDS-PAGE gels. For single-molecule work, the technique also has particular relevance for the labelling of membrane-bound receptor proteins[258, 259], as well as proteins in sub-cellular compartments[260, 261]. A number of live-cell based applications have also highlighted protein tags and applications range from super-resolution imaging[262], measuring protein activity[263, 264], determining interactions via FRET[265] and particle tracking[266].

An alternative to the SNAP/CLIP approach is the use of the HaloTag (**Figure 9d**), a 33kDa derivative of a bacterial haloalkane dehalogenase enzyme[267] which forms an irreversible covalent bond between the fused protein and the HaloTag ligand upon binding[268]. Here, a transient alkyl-enzyme intermediate is formed during the displacement of a terminal chloride with Asp106, and since His272 does not catalyse the hydrolysis, a stable covalent bond is formed[267]. Much like the SNAP and CLIP tags, only a single genetic construct is required and most are fused directly to the C- or N-terminus, but in contrast, the HaloTag can be used under relatively acidic conditions, opening possibilities for its utility in harsh microenvironments[269].

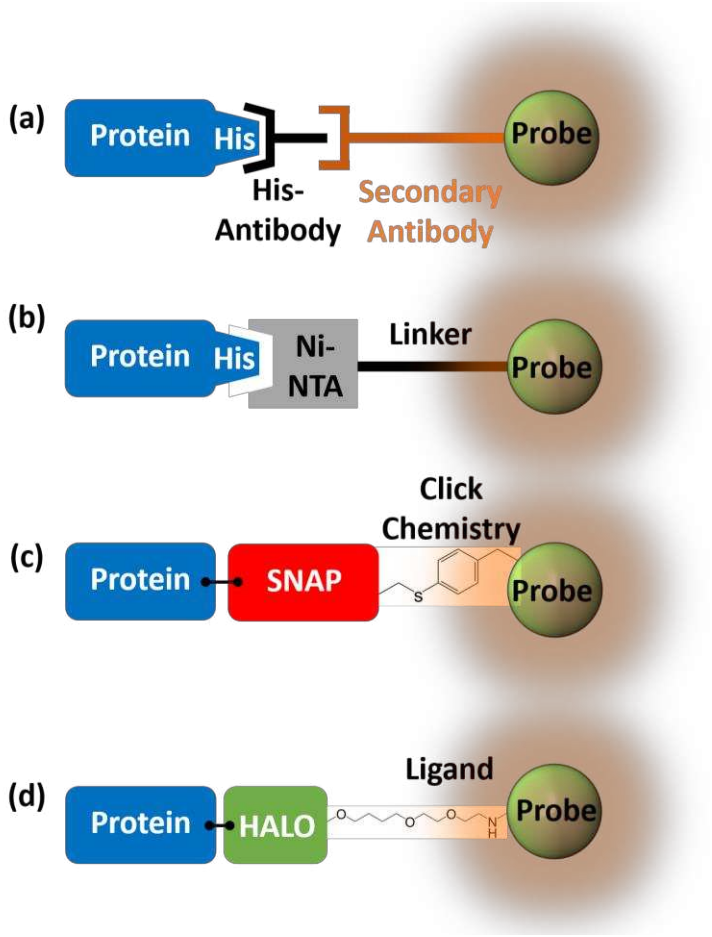

Figure 9. Comparison of protein labelling methods involving protein tags. Schematic illustrations of (a) conventional His-tag antibody coupling, (b) Ni-NTA-linker conjugation, (c) SNAP-tag and (d) HALO-tag labelling.

Alternative specific labeling strategies involving tetracysteine tags can be used if the methods listed above are unavailable. This approach involves the binding of the membrane permeable fluorescein derivative FlAsH or resofurin derivative ReAsH, to a peptide sequence of the form C-C-X-X-C-C, where C represents Cysteine and X denotes any amino acid[270, 271]. The recognition sequence is typically inserted into solvent accessible, looped or disordered regions on the protein of interest. Both fluorophores are non-emissive in the unbound state and become emissive upon conjugation. This technique has been applied extensively in vitro and in cellulo to a range of biological questions including but not limited to single-molecule protein dynamics[272] and protein aggregation[273].

4. Enhancing Photostability

Two major problems for single-molecule studies utilizing fluorescent probes are photobleaching and photoblinking. In recent years, the community has made major advances towards solving these problems and a host of novel anti-fading agents have been tested and developed to decrease the rates of bleaching and blinking. Here, we discuss the most popular choices of oxygen scavengers and triplet state quenchers with emphasis placed on their relative benefits.

In the case of photobleaching, the fluorescent probe enters an irreversible non-emissive dark state which limits the time window over which individual molecules can be studied. When photoblinking occurs, reversible transitions to long-lived and non-radiative dark-states complicates, for example, particle tracking and FRET measurements. While the mechanisms by which photobleaching and photoblinking are not entirely defined, and are fluorophore-dependent, it is recognised that molecular oxygen plays a substantial role in the formation of non-emissive states, either via direct interaction with the fluorophore or indirectly by producing free radicals in solution. Consequently, many single-molecule investigations utilizing organic dyes have incorporated the use of oxygen scavengers such as chromatin, cyclooctatetraene, 4-nitrobenzyl alcohol and l-ascorbic acid, either covalently attached to the probe of interest or in free solution[274, 275]. However, effectively minimizing molecular oxygen through physical means is challenging and so enzymatic oxygen scavengers are commonly employed instead. For example, the combination of D-glucose, glucose oxidase and catalase can reduce the molecular oxygen concentration via the coupled reactions though we note use of this system can lead to subtle pH reductions[276]. An alternative strategy making use of protocatechuate-3,4-dioxygenase, protocatechuic acid, pyranose oxidase, catalase and glucose can further reduce molecular oxygen levels[277]. Furthermore, the addition of the vitamin E analogue 6-hydroxy-2,5,7,8-tetramethylchromane-2-carboxylic acid (Trolox) minimizes photoblinking through a mechanism that involves suppressing the triplet state through electron transfer and recovery of the resulting radical ion by the complementary redox reactions[278].

Unfortunately, the protection from photoblinking and photobleaching provided by this cocktail is non-existent for fluorescent proteins. To mitigate against this, researchers have often minimized light exposure and/or the sampling frequency, and typically choose fluorescent proteins which are most photostable[279, 280]. Careful selection of cell imaging media with selected vitamins (riboflavin and pyridoxal) removed has been found to decrease the photobleaching of GFP relative to conventional buffer solutions while maintaining cell function[281], and though a number of commercial anti-fade media exist, each is likely to be fluorophore- and cell-dependent.

Fluorescence intermittency has also been universally observed from quantum dots and this of course be a major limitation for long term imaging or tracking experiments. In specific cases, surface passivation of core-shell CdSe/ZnS quantum dots with short chain length thiol moieties was found to suppress photoblinking[282]. Similarly, indium tin oxide nanoparticles suppressed the blinking of CdSeTe/ZnS core-shell quantum dots[283], though we note that these results are not generalizable to all types of quantum dot. Further experiments demonstrated that surface-modification of core-type CdTe quantum dots with gadolinium ions promotes blinking, which could find useful utility in super-resolution applications[171].

Other strategies of enhancing photostability, which do not rely on a chemical cocktail, include the fluorination of dyes at the synthesis stage. Polyfluorinated cyanine derivatives upon comparison with non-fluorinated analogues for instance, were found to display at least a 10-fold reduction in aggregation, > 10% increase in quantum yield, and 4-fold greater resistance to photobleaching due to reduced reactivity towards singlet oxygen. Clearly, all are extremely attractive for single-molecule applications, and are generally attributed to the fluorination of the benzothiazole heterocycles[284]. More recently, organic dyes containing a perfluorophenyl group have also attracted attention because of their enhanced photostability and optical properties. In this regard, ring-perfluorinated trimethine cyanines have been shown to display almost a two-fold higher fluorescence quantum yield and lifetime, and 2.5-fold lower nonradiative deactivation rate constant compared with the nonfluorinated version[285]. Other strategies to improve photostability involve introducing electron-deficient substituents to reduce the overall reactivity of the probe toward singlet oxygen[286], conjugation of the probe

to a triplet state quencher[287], non-covalent encapsulation of the probe into a charged copolymer[288] or nanoparticle[289], or through nanohybrid formation[290].

In most applications, removal of photobleaching is desirable. However we note that in the case of single-molecule stepwise photobleaching analysis, where the stoichiometry of a complex containing labelled sub-units is estimated based on the number of photobleaching events[291], both the labelling and detection efficiencies are critical for accurate estimations[292].

Single-molecule fluorescence methods are increasingly used across the chemical, biological and medical sciences, and a growing interest is developing in near-infrared fluorophores as imaging probes, in part because they enable deeper imaging through organic material compared with shorter wavelength probes but also because they generally facilitate higher signal-to-noise ratios due to lower autofluorescence at longer wavelengths. Considering this, the incorporation of oligoglycerol dendrons into such probes has enabled additional improvements in photostability in vitro and within living cells relative to conventional cyanines, suggesting this approach may well also be applicable for improving the photostability of a wide range of hydrophobic aromatic probes[293].

5. Single-Molecule Fluorescence Detection

Parallel developments in probe designs, experimental techniques and computational methods have given rise to a new series of multiplexed, correlative technologies capable of tackling previously intractable biological questions[35]. Improvements in the sensitivity and speed of detectors, the efficiency and stability of excitation sources and microfluidics have all played a role in the development of tools and techniques capable of detecting and manipulating single fluorescently-labelled biomolecules at work. While it is out with the scope of this review to list and describe them all, these transformative technologies, which include, but are not limited to TIRF microscopy[294], confocal-based multi-parameter fluorescence detection[295], a suite of super-resolution methods[144, 296, 297] and fluorescence-integrated optical and magnetic based manipulation tools[298], are contributing enormously to answering long-standing biological questions[299]. At the heart of this is the development of single-molecule probes, without which these fundamental biological processes and functions would remain, for the most part, invisible.

Most single-molecule measurements are performed in biologically relevant solutions, with the target molecule either tethered to a surface or allowed to freely diffuse. In the former case, the most common immobilization strategy involves the tethering of the biomolecule of interest to a surface via biotin-streptavidin interactions, as schematically shown in **Figure 4d**. Here, mixing of a passivation reagent with its biotinylated counterpart and addition of Avidin allows the immobilization of biotinylated molecules via a biotin-avidin linkage with high specificity and affinity ($k_d \sim 10^{-15}$ M) [50]. Alternative approaches include the use of covalent-bond based click-chemistry[300], encapsulation within lipid vesicles[301], non-specific electrostatic interactions with an adsorbed passivation layer[302] or immobilization within a gel[303] however in all cases, care must be taken to ensure the immobilization scheme does not hinder biological function and the probe does not interact with the surface. This issue is in part bypassed by detecting freely-diffusing biomolecules, though the measurement window is limited by the time spent transiting through the excitation volume. For a typical confocal based measurement, it is not uncommon for biomolecules to diffuse away from the excitation source within several milliseconds. On the flip side, this also affords an opportunity to gain access to diffusion coefficients and hydrodynamic radii via fluorescence fluctuation correlation spectroscopy and use of the Stokes-Einstein equation[304-306].

In nearly all cases, and irrespective of the detection scheme used, maximizing the available photon budget, and the signal-to- noise ratio is critical for single-molecule detection, especially when sub-millisecond temporal resolution is required. Clearly, this goes hand-in-hand with the need to ensure abundance of the molecule of interest, and a protocol for high labelling efficiency. Nevertheless, this concern ultimately drives the need for brighter and more photostable probes to prolong observation time windows and increase the number of collected photons. While several analytical algorithms have been tailored towards improving the signal-to-noise ratio post-acquisition[307, 308], and probe-free techniques, such as digital holographic[309] and interferometric scattering[310] microscopy are emerging as promising tools for exploring biomolecular function, the requirement to obtain fluorescent probes with quantum yields approaching unity, whilst remaining minimally perturbing, remains an active and critical area of research.

Combining research efforts in a range of these different approaches, such as the engineering of new fluorescent probes with enhanced photostability, minimizing background fluorescence, and improving the sensitivity of detectors, will continue to aid maximization of the available photon signal. However, single-molecule experiments are not without limitations. For instance, low signal-to-noise ratios are often observed when fast acquisition rates are used and there is an intrinsic requirement for using the probes under dilute conditions. While a number of analytical tools[3, 306, 311] have recently been developed to combat the signal-to-noise problem, essentially enabling otherwise hidden information to be obtained from millisecond sampled images, the latter limits the detection scheme to less than a few nanomolar, even when localized excitation is used. Indeed, localization microscopy and particle tracking perform badly if fluorophores are close together in the sample and the limiting concentration depends on the spatial dimensionality of the tagged biomolecule, its mobility, and ability to cluster. While labelling a sub-population can get the concentration of fluorescent species below this limit, the method yields a significant proportion of unlabelled species in the sample, and many of these may potentially have different physical properties to the tagged species. An alternative strategy involves delimited photobleaching whereby a fraction of the fluorophore population is photobleached for a given period prior to localization microscopy. Unfortunately, both methods produce a substantial ‘dark’ population of the biomolecule under investigation. In this regard, the development of photoactivatable probes has been used in many cases to help alleviate the issue and extend the concentration range for analysis. Super-resolution methods, including photoactivated localization microscopy (PALM) and single-particle tracking make use of such probes to facilitate investigations into the organization and localization of diffraction-limited fluorescent species in living cells with a density of molecules high enough to provide structural context. When the two methods are combined, information is gained on the positions of single-molecules by activating, localizing and bleaching subsets of for instance, photoactivatable fluorescent proteins[312]. In this regard, we steer the reader to comprehensive reviews[313-317] that discuss such approaches, mechanisms of photoactivation, and advantages and limitations of photoactivatable probe designs.

Carefully applied, the combination of single-molecule fluorescent probes, labelling strategy, and immobilization and detection scheme provides a strong platform for understanding the complexities of life’s biomolecules in far greater detail than ever before.

6. Final Notes

New and exciting technical developments over the last few decades, even those currently at proof-of-principle stage offer the modern multidisciplinary researcher a wealth of opportunity for characterizing single biomolecules in action, one-at-a-time, bypassing limitations associated with conventional ensemble averaging. Spectroscopic methods that employ single-

molecule fluorescent probes, from particle tracking to FRET, not only complement structural and functional characterization methods, but offer the ability to observe time-dependent, and often, heterogeneous interactions.

The ideal experimental toolbox allowing efficient applications of single-molecule techniques in complex biomolecular systems comprises two major factors: (i) the appropriately selected fluorescent probe(s), which should have sufficient spectroscopic and molecular properties, and (ii) a corresponding, appropriately designed, conjugation scheme. Developments in probe design, coupled with new site-specific labelling procedures, now provide the single-molecule community with a facile yet robust platform for quantitative analyses across a huge range of biomolecules and experimental situations.

Undoubtedly there are many hurdles yet to overcome. For example, the general issues of increasing probe brightness and photostability; the broader application of single-molecule fluorescent probes for environmental sensing; the requirement to develop minimally invasive labelling schemes; the need for specific targeting of biomolecules within a biological soup; and the need to detect sensitive and transient interactions.

The potential of single-molecule techniques cannot be underestimated, and with new and emerging fluorescent probe designs, the promise of this field is vast. The opportunities presented by combining fluorescence sensing, imaging and spectroscopic tools with each other, and indeed with others such as atomic force and cryo-electron microscopy, for example, could lead to revolutionary biological insights by unmasking currently intractable information and interactions. In short, fluorescent probes with optimum properties combined with appropriate conjugation strategies are essential for high-quality and insightful single-molecule fluorescence measurements. Small fluorescent probes enable access to the nanoworld and they are helping to resolve our understanding of the biological jigsaw puzzle piece-by-piece. As probe designs evolve further and their applications broaden, fresh ideas and questions will emerge, stimulating the next-generation of modern single-molecule biophysical experiments.

7. Acknowledgements

ML was supported by BBSRC (grant refs. BB/R001235/1 and BB/P000746/1) and EPSRC (grant ref. EP/T002166/1). SQ was supported by Alzheimer's Research UK (grant ref. ARUK-RF2019A-001). The authors would like to thank Dr. Sviatlana Shashkova (University of York, UK) for providing the images shown in Figure 5a, Dr. George D. Watson and Dr. Agnes Noy (both University of York, UK) for performing the molecular dynamics simulation shown in Figure 4a, and Dr. Ben Ambrose (University of Sheffield, UK) for performing the modelling shown in Figure 8d.

8. References

1. Miller H, Zhou Z, Shepherd J, Wollman AJM, Leake MC. Single-molecule techniques in biophysics: a review of the progress in methods and applications. Rep Prog Phys. 2018;81(2):024601.
2. Harriman OLJ, Leake MC. Single molecule experimentation in biological physics: exploring the living component of soft condensed matter one molecule at a time. J Phys-Condens Mat. 2011;23(50).
3. Leake MC. Analytical tools for single-molecule fluorescence imaging in cellulo. Phys Chem Chem Phys. 2014;16(25):12635-47.
4. Leake MC. The physics of life: one molecule at a time. Philos T R Soc B. 2013;368(1611).
5. Moerner WE, Kador L. Optical-Detection and Spectroscopy of Single Molecules in a Solid. Phys Rev Lett. 1989;62(21):2535-8.

6. Orrit M, Bernard J. Single Pentacene Molecules Detected by Fluorescence Excitation in a Para-Terphenyl Crystal. Phys Rev Lett. 1990;65(21):2716-9.
7. Moerner WE. New directions in single-molecule imaging and analysis. P Natl Acad Sci USA. 2007;104(31):12596-602.
8. Vale RD, Funatsu T, Pierce DW, Romberg L, Harada Y, Yanagida T. Direct observation of single kinesin molecules moving along microtubules. Nature. 1996;380(6573):451-3.
9. Ha TJ, Ting AY, Liang J, Caldwell WB, Deniz AA, Chemla DS, et al. Single-molecule fluorescence spectroscopy of enzyme conformational dynamics and cleavage mechanism. P Natl Acad Sci USA. 1999;96(3):893-8.
10. Lu HP, Xun LY, Xie XS. Single-molecule enzymatic dynamics. Science. 1998;282(5395):1877-82.
11. Noji H, Yasuda R, Yoshida M, Kinosita K. Direct observation of the rotation of F-1-ATPase. Nature. 1997;386(6622):299-302.
12. Bopp MA, Sytnik A, Howard TD, Cogdell RJ, Hochstrasser RM. The dynamics of structural deformations of immobilized single light-harvesting complexes. P Natl Acad Sci USA. 1999;96(20):11271-6.
13. Hwang H, Myong S. Protein induced fluorescence enhancement (PIFE) for probing protein-nucleic acid interactions. Chem Soc Rev. 2014;43(4):1221-9.
14. Xie Z, Srividya N, Sosnick TR, Pan T, Scherer NF. Single-molecule studies highlight conformational heterogeneity in the early folding steps of a large ribozyme. P Natl Acad Sci USA. 2004;101(2):534-9.
15. Leake MC, Chandler JH, Wadhams GH, Bai F, Berry RM, Armitage JP. Stoichiometry and turnover in single, functioning membrane protein complexes. Nature. 2006;443(7109):355-8.
16. Reyes-Lamothe R, Sherratt DJ, Leake MC. Stoichiometry and Architecture of Active DNA Replication Machinery in Escherichia coli. Science. 2010;328(5977):498-501.
17. Syeda AH, Wollman AJM, Hargreaves AL, Howard JAL, Bruning JG, McGlynn P, et al. Single-molecule live cell imaging of Rep reveals the dynamic interplay between an accessory replicative helicase and the replisome. Nucleic Acids Res. 2019;47(12):6287-98.
18. Stracy M, Wollman AJM, Kaja E, Gapinski J, Lee JE, Leek VA, et al. Single-molecule imaging of DNA gyrase activity in living Escherichia coli. Nucleic Acids Res. 2019;47(1):210-20.
19. Hollars CW, Dunn RC. Probing single molecule orientations in model lipid membranes with near-field scanning optical microscopy. J Chem Phys. 2000;112(18):7822-30.
20. Talley CE, Dunn RC. Single molecules as probes of lipid membrane microenvironments. J Phys Chem B. 1999;103(46):10214-20.
21. Dresser L, Graham SP, Miller LM, Schaefer C, Conteduca D, Johnson S, et al. Tween-20 Induces the Structural Remodeling of Single Lipid Vesicles. J Phys Chem Lett. 2022:5341-50.
22. Sako Y, Minoguchi S, Yanagida T. Single-molecule imaging of EGFR signalling on the surface of living cells. Nat Cell Biol. 2000;2(3):168-72.
23. Wang SZ, Vafabakhsh R, Borschell WF, Ha T, Nichols CG. Structural dynamics of potassium-channel gating revealed by single-molecule FRET. Nat Struct Mol Biol. 2016;23(1):31-6.
24. Roy R, Hohng S, Ha T. A practical guide to single-molecule FRET. Nat Methods. 2008;5(6):507-16.
25. Wu L, Huang C, Emery BP, Sedgwick AC, Bull SD, He XP, et al. Forster resonance energy transfer (FRET)-based small-molecule sensors and imaging agents. Chem Soc Rev. 2020;49(15):5110-39.
26. Baltierra-Jasso LE, Morten MJ, Laflor L, Quinn SD, Magennis SW. Crowding-Induced Hybridization of Single DNA Hairpins. J Am Chem Soc. 2015;137(51):16020-3.
27. Paudel BP, Rueda D. Molecular Crowding Accelerates Ribozyme Docking and Catalysis. J Am Chem Soc. 2014;136(48):16700-3.
28. Scharfen L, Schlierf M. Real-time monitoring of protein-induced DNA conformational changes using single-molecule FRET. Methods. 2019;169:11-20.

29. Schuler B. Single-molecule FRET of protein structure and dynamics - a primer. J Nanobiotechnol. 2013;11.
30. Diez M, Zimmermann B, Borsch M, Konig M, Schweinberger E, Steigmiller S, et al. Proton-powered subunit rotation in single membrane-bound F0F1-ATP synthase. Nat Struct Mol Biol. 2004;11(2):135-41.
31. Kalinin S, Peulen T, Sindbert S, Rothwell PJ, Berger S, Restle T, et al. A toolkit and benchmark study for FRET-restrained high-precision structural modeling. Nat Methods. 2012;9(12):1218-U129.
32. Dimura M, Peulen TO, Hanke CA, Prakash A, Gohlke H, Seidel CAM. Quantitative FRET studies and integrative modeling unravel the structure and dynamics of biomolecular systems. Curr Opin Struc Biol. 2016;40:163-85.
33. Hellenkamp B, Schmid S, Doroshenko O, Opanasyuk O, Kuhnemuth R, Adariani SR, et al. Precision and accuracy of single-molecule FRET measurements-a multi-laboratory benchmark study. Nat Methods. 2018;15(9):669-+.
34. Chen J, Tsai A, Petrov A, Puglisi JD. Nonfluorescent Quenchers To Correlate Single-Molecule Conformational and Compositional Dynamics. J Am Chem Soc. 2012;134(13):5734-7.
35. Hoffman DP, Shtengel G, Xu CS, Campbell KR, Freeman M, Wang L, et al. Correlative three-dimensional super-resolution and block-face electron microscopy of whole vitreously frozen cells. Science. 2020;367(6475).
36. Holden SJ, Uphoff S, Hohlbein J, Yadin D, Le Reste L, Britton OJ, et al. Defining the Limits of Single-Molecule FRET Resolution in TIRF Microscopy. Biophys J. 2010;99(9):3102-11.
37. Kondo T, Chen WJ, Schlau-Cohen GS. Single-Molecule Fluorescence Spectroscopy of Photosynthetic Systems. Chem Rev. 2017;117(2):860-98.
38. Shroder DY, Lippert LG, Goldman YE. Single molecule optical measurements of orientation and rotations of biological macromolecules. Methods Appl Fluoresc. 2016;4(4):042004.
39. Valades Cruz CA, Shaban HA, Kress A, Bertaux N, Monneret S, Mavrakis M, et al. Quantitative nanoscale imaging of orientational order in biological filaments by polarized superresolution microscopy. Proc Natl Acad Sci U S A. 2016;113(7):E820-8.
40. van Mameren J, Vermeulen K, Wuite GJL, Peterman EJG. A polarized view on DNA under tension. J Chem Phys. 2018;148(12):123306.
41. Backer AS, Biebricher AS, King GA, Wuite GJL, Heller I, Peterman EJG. Single-molecule polarization microscopy of DNA intercalators sheds light on the structure of S-DNA. Sci Adv. 2019;5(3):eaav1083.
42. Stevens BC, Ha T. Discrete and heterogeneous rotational dynamics of single membrane probe dyes in gel phase supported lipid bilayer. J Chem Phys. 2004;120(6):3030-9.
43. Sun Y, Sato O, Ruhnow F, Arsenault ME, Ikebe M, Goldman YE. Single-molecule stepping and structural dynamics of myosin X. Nat Struct Mol Biol. 2010;17(4):485-91.
44. Shepherd JW, Payne-Dwyer AL, Lee JE, Syeda A, Leake MC. Combining single-molecule super-resolved localization microscopy with fluorescence polarization imaging to study cellular processes. J Phys-Photonics. 2021;3(3).
45. Hoogenboom BW, Leake MC. The case for biophysics super-groups in physics departments. Phys Biol. 2018;15(6).
46. Zheng QS, Juette MF, Jockusch S, Wasserman MR, Zhou Z, Altman RB, et al. Ultra-stable organic fluorophores for single-molecule research. Chem Soc Rev. 2014;43(4):1044-56.
47. Ha T, Tinnefeld P. Photophysics of Fluorescent Probes for Single-Molecule Biophysics and Super-Resolution Imaging. Annu Rev Phys Chem. 2012;63:595-617.
48. Lee J, Lee S, Ragunathan K, Joo C, Ha T, Hohng S. Single-Molecule Four-Color FRET. Angew Chem Int Edit. 2010;49(51):9922-5.
49. Toseland CP. Fluorescent labeling and modification of proteins. J Chem Biol. 2013;6(3):85-95.
50. Gust A, Zander A, Gietl A, Holzmeister P, Schulz S, Lalkens B, et al. A Starting Point for Fluorescence-Based Single-Molecule Measurements in Biomolecular Research. Molecules. 2014;19(10):15824-65.

51. Fu YH, Finney NS. Small-molecule fluorescent probes and their design. Rsc Adv. 2018;8(51):29051-61.
52. Shim SH, Xia C, Zhong G, Babcock HP, Vaughan JC, Huang B, et al. Super-resolution fluorescence imaging of organelles in live cells with photoswitchable membrane probes. Proc Natl Acad Sci U S A. 2012;109(35):13978-83.
53. Staffend NA, Meisel RL. DiOlistic labeling of neurons in tissue slices: a qualitative and quantitative analysis of methodological variations. Front Neuroanat. 2011;5.
54. Yoon TY, Okumus B, Zhang F, Shin YK, Ha T. Multiple intermediates in SNARE-induced membrane fusion. Proc Natl Acad Sci U S A. 2006;103(52):19731-6.
55. Lehmann TP, Juzwa W, Filipiak K, Sujka-Kordowska P, Zabel M, Glowacki J, et al. Quantification of the asymmetric migration of the lipophilic dyes, DiO and DiD, in homotypic co-cultures of chondrosarcoma SW-1353 cells. Mol Med Rep. 2016;14(5):4529-36.
56. Hofmann MH, Bleckmann H. Effect of temperature and calcium on transneuronal diffusion of DiI in fixed brain preparations. J Neurosci Methods. 1999;88(1):27-31.
57. Packard BS, Wolf DE. Fluorescence lifetimes of carbocyanine lipid analogues in phospholipid bilayers. Biochemistry. 1985;24(19):5176-81.
58. Hu Y, Tian Z, Diao J. Single-Molecule Fluorescence Measurement of SNARE-Mediated Vesicle Fusion. Methods Mol Biol. 2019;1860:335-44.
59. Machado R, Bendesky J, Brown M, Spendier K, Hagen GM. Imaging Membrane Curvature inside a FcepsilonRI-Centric Synapse in RBL-2H3 Cells Using TIRF Microscopy with Polarized Excitation. J Imaging. 2019;5(7).
60. De Proost I, Pintelon I, Wilkinson WJ, Goethals S, Brouns I, Van Nassauw L, et al. Purinergic signaling in the pulmonary neuroepithelial body microenvironment unraveled by live cell imaging. FASEB J. 2009;23(4):1153-60.
61. Van Haeften T, Wouterlood FG. Neuroanatomical tracing at high resolution. J Neurosci Meth. 2000;103(1):107-16.
62. Diao J, Su Z, Ishitsuka Y, Lu B, Lee KS, Lai Y, et al. A single-vesicle content mixing assay for SNARE-mediated membrane fusion. Nat Commun. 2010;1:54.
63. Dalgarno PA, Juan-Colas J, Hedley GJ, Pineiro L, Novo M, Perez-Gonzalez C, et al. Unveiling the multi-step solubilization mechanism of sub-micron size vesicles by detergents. Sci Rep. 2019;9(1):12897.
64. Juan-Colas J, Dresser L, Morris K, Lagadou H, Ward RH, Burns A, et al. The Mechanism of Vesicle Solubilization by the Detergent Sodium Dodecyl Sulfate. Langmuir. 2020;36(39):11499-507.
65. Zheng QS, Lavis LD. Development of photostable fluorophores for molecular imaging. Curr Opin Chem Biol. 2017;39:32-8.
66. Grimm JB, Lavis LD. Synthesis of Rhodamines from Fluoresceins Using Pd-Catalyzed C-N Cross-Coupling. Org Lett. 2011;13(24):6354-7.
67. Grimm JB, English BP, Chen JJ, Slaughter JP, Zhang ZJ, Revyakin A, et al. A general method to improve fluorophores for live-cell and single-molecule microscopy. Nat Methods. 2015;12(3):244-+.
68. Swinstead EE, Miranda TB, Paakinaho V, Baek S, Goldstein I, Hawkins M, et al. Steroid Receptors Reprogram FoxA1 Occupancy through Dynamic Chromatin Transitions. Cell. 2016;165(3):593-605.
69. Bisson AW, Hsu YP, Squyres GR, Kuru E, Wu FB, Jukes C, et al. Treadmilling by FtsZ filaments drives peptidoglycan synthesis and bacterial cell division. Science. 2017;355(6326):739-43.
70. Arden-Jacob J, Frantzeskos J, Kemnitzer NU, Zilles A, Drexhage KH. New fluorescent markers for the red region. Spectrochim Acta A. 2001;57(11):2271-83.
71. Koide Y, Urano Y, Hanaoka K, Terai T, Nagano T. Evolution of Group 14 Rhodamines as Platforms for Near-Infrared Fluorescence Probes Utilizing Photoinduced Electron Transfer. Acs Chem Biol. 2011;6(6):600-8.

72. Lukinavicius G, Umezawa K, Olivier N, Honigmann A, Yang GY, Plass T, et al. A near-infrared fluorophore for live-cell super-resolution microscopy of cellular proteins. Nat Chem. 2013;5(2):132-9.
73. Dvivedi A, Rajakannu P, Ravikanth M. meso-Salicylaldehyde substituted BODIPY as a chemodosimetric sensor for cyanide anions. Dalton T. 2015;44(9):4054-62.
74. Sadoine M, Cerminara M, Gerrits M, Fitter J, Katranidis A. Cotranslational Incorporation into Proteins of a Fluorophore Suitable for smFRET Studies. Acs Synth Biol. 2018;7(2):405-11.
75. Zanetti-Domingues LC, Tynan CJ, Rolfe DJ, Clarke DT, Martin-Fernandez M. Hydrophobic Fluorescent Probes Introduce Artifacts into Single Molecule Tracking Experiments Due to Non-Specific Binding. Plos One. 2013;8(9).
76. Woolhead CA, McCormick PJ, Johnson AE. Nascent membrane and secretory proteins differ in FRET-detected folding far inside the ribosome and in their exposure to ribosomal proteins. Cell. 2004;116(5):725-36.
77. Holtkamp W, Kokic G, Jager M, Mittelstaet J, Komar AA, Rodnina MV. Cotranslational protein folding on the ribosome monitored in real time. Science. 2015;350(6264):1104-7.
78. Schweighofer F, Dworak L, Hammer CA, Gustmann H, Zastrow M, Ruck-Braun K, et al. Highly efficient modulation of FRET in an orthogonally arranged BODIPY-DTE dyad. Sci Rep-Uk. 2016;6.
79. Shao JY, Sun HY, Guo HM, Ji SM, Zhao JZ, Wu WT, et al. A highly selective red-emitting FRET fluorescent molecular probe derived from BODIPY for the detection of cysteine and homocysteine: an experimental and theoretical study. Chem Sci. 2012;3(4):1049-61.
80. Jin T, Garcia-Lopez V, Chen F, Tour J, Wang GF. Imaging Single Molecular Machines Attached with Two BODIPY Dyes at the Air-Solid Interface: High Probability of Single-Step-Like Photobleaching and Nonscaling Intensity. J Phys Chem C. 2016;120(46):26522-31.
81. Berlier JE, Rothe A, Buller G, Bradford J, Gray DR, Filanoski BJ, et al. Quantitative comparison of long-wavelength Alexa Fluor dyes to Cy dyes: Fluorescence of the dyes and their bioconjugates. J Histochem Cytochem. 2003;51(12):1699-712.
82. Chao J, Ram S, Ward ES, Ober RJ. Ultrahigh accuracy imaging modality for super-localization microscopy. Nat Methods. 2013;10(4):335-+.
83. Marsh RJ, Pfisterer K, Bennett P, Hirvonen LM, Gautel M, Jones GE, et al. Artifact-free high-density localization microscopy analysis. Nat Methods. 2018;15(9):689-+.
84. Kasper R, Harke B, Forthmann C, Tinnefeld P, Hell SW, Sauer M. Single-Molecule STED Microscopy with Photostable Organic Fluorophores. Small. 2010;6(13):1379-84.
85. Dalton CE, Quinn SD, Rafferty A, Morten MJ, Gardiner JM, Magennis SW. Single-Molecule Fluorescence Detection of a Synthetic Heparan Sulfate Disaccharide. Chemphyschem. 2016;17(21):3442-6.
86. Letschert S, Gohler A, Franke C, Bertleff-Zieschang N, Memmel E, Doose S, et al. Super-Resolution Imaging of Plasma Membrane Glycans. Angew Chem Int Edit. 2014;53(41):10921-4.
87. Jiang H, English BP, Hazan RB, Wu P, Ovryn B. Tracking Surface Glycans on Live Cancer Cells with Single-Molecule Sensitivity. Angew Chem Int Edit. 2015;54(6):1765-9.
88. Kim E, Lee S, Jeon A, Choi JM, Lee HS, Hohng S, et al. A single-molecule dissection of ligand binding to a protein with intrinsic dynamics. Nat Chem Biol. 2013;9(5):313-+.
89. Kaur G, Lewis JS, van Oijen AM. Shining a Spotlight on DNA: Single-Molecule Methods to Visualise DNA. Molecules. 2019;24(3).
90. Morikawa K, Yanagida M. Visualization of Individual DNA-Molecules in Solution by Light-Microscopy - Dapi Staining Method. J Biochem-Tokyo. 1981;89(2):693-6.
91. Reuter M, Dryden DTF. The kinetics of YOYO-1 intercalation into single molecules of double-stranded DNA. Biochem Bioph Res Co. 2010;403(2):225-9.
92. Stanojcic S, Kuk N, Ullah I, Sterkers Y, Merrick CJ. Single-molecule analysis reveals that DNA replication dynamics vary across the course of schizogony in the malaria parasite Plasmodium falciparum. Sci Rep-Uk. 2017;7.

93. Backer AS, Biebricher AS, King GA, Wuite GJL, Heller I, Peterman EJG. Single-molecule polarization microscopy of DNA intercalators sheds light on the structure of S-DNA. Sci Adv. 2019;5(3).
94. Yan XM, Habbersett RC, Cordek JM, Nolan JP, Yoshida TM, Jett JH, et al. Development of a mechanism-based, DNA staining protocol using SYTOX orange nucleic acid stain and DNA fragment sizing flow cytometry. Anal Biochem. 2000;286(1):138-48.
95. Yan XM, Habbersett RC, Yoshida TM, Nolan JP, Jett JH, Marrone BL. Probing the kinetics of SYTOX orange stain binding to double-stranded DNA with implications for DNA analysis. Anal Chem. 2005;77(11):3554-62.
96. Collins BE, Ye LF, Duzdevich D, Greene EC. DNA curtains: Novel tools for imaging protein-nucleic acid interactions at the single-molecule level. Method Cell Biol. 2014;123:217-34.
97. Almaqwashi AA, Paramanathan T, Rouzina I, Williams MC. Mechanisms of small molecule-DNA interactions probed by single-molecule force spectroscopy. Nucleic Acids Res. 2016;44(9):3971-88.
98. Paramanathan T, Vladescu I, McCauley MJ, Rouzina I, Williams MC. Force spectroscopy reveals the DNA structural dynamics that govern the slow binding of Actinomycin D. Nucleic Acids Research. 2012;40(11):4925-32.
99. Miller H, Zhou ZK, Wollman AJM, Leake MC. Superresolution imaging of single DNA molecules using stochastic photoblinking of minor groove and intercalating dyes. Methods. 2015;88:81-8.
100. Sischka A, Toensing K, Eckel R, Wilking SD, Sewald N, Ros R, et al. Molecular mechanisms and kinetics between DNA and DNA binding ligands. Biophys J. 2005;88(1):404-11.
101. Murade CU, Subramaniam V, Otto C, Bennink ML. Interaction of Oxazole Yellow Dyes with DNA Studied with Hybrid Optical Tweezers and Fluorescence Microscopy. Biophys J. 2009;97(3):835-43.
102. Gunther K, Mertig M, Seidel R. Mechanical and structural properties of YOYO-1 complexed DNA. Nucleic Acids Res. 2010;38(19):6526-32.
103. Biebricher AS, Heller I, Roijmans RFH, Hoekstra TP, Peterman EJG, Wuite GJL. The impact of DNA intercalators on DNA and DNA-processing enzymes elucidated through force-dependent binding kinetics. Nat Commun. 2015;6.
104. Carter KP, Young AM, Palmer AE. Fluorescent Sensors for Measuring Metal Ions in Living Systems. Chem Rev. 2014;114(8):4564-601.
105. Walkup GK, Burdette SC, Lippard SJ, Tsien RY. A new cell-permeable fluorescent probe for Zn2+. J Am Chem Soc. 2000;122(23):5644-5.
106. Nolan EM, Lippard SJ. Small-Molecule Fluorescent Sensors for Investigating Zinc Metalloneurochemistry. Accounts Chem Res. 2009;42(1):193-203.
107. Hirano T, Kikuchi K, Urano Y, Nagano T. Improvement and biological applications of fluorescent probes for zinc, ZnAFs. J Am Chem Soc. 2002;124(23):6555-62.
108. Gee KR, Zhou ZL, Ton-That D, Sensi SL, Weiss JH. Measuring zinc in living cells. A new generation of sensitive and selective fluorescent probes. Cell Calcium. 2002;31(5):245-51.
109. Zalewski PD, Forbes IJ, Betts WH. Correlation of Apoptosis with Change in Intracellular Labile Zn(Ii) Using Zinquin [(2-Methyl-8-P-Toluenesulphonamido-6-Quinolyloxy)Acetic Acid], a New Specific Fluorescent-Probe for Zn(Ii). Biochem J. 1993;296:403-8.
110. Que EL, Bleher R, Duncan FE, Kong BY, Gleber SC, Vogt S, et al. Quantitative mapping of zinc fluxes in the mammalian egg reveals the origin of fertilization-induced zinc sparks. Nat Chem. 2015;7(2):130-9.
111. Rivera-Fuentes P, Lippard SJ. SpiroZin1: A Reversible and pH-Insensitive, Reaction-Based, Red-Fluorescent Probe for Imaging Biological Mobile Zinc. Chemmedchem. 2014;9(6):1238-43.
112. Rivera-Fuentes P, Wrobel AT, Zastrow ML, Khan M, Georgiou J, Luyben TT, et al. A far-red emitting probe for unambiguous detection of mobile zinc in acidic vesicles and deep tissue. Chem Sci. 2015;6(3):1944-8.

113. Han Y, Goldberg JM, Lippard SJ, Palmer AE. Superiority of SpiroZin2 Versus FluoZin-3 for monitoring vesicular Zn2+ allows tracking of lysosomal Zn2+ pools. Sci Rep-Uk. 2018;8.
114. Tsien RY, Pozzan T, Rink TJ. T-Cell Mitogens Cause Early Changes in Cytoplasmic Free Ca(2+) and Membrane-Potential in Lymphocytes. Nature. 1982;295(5844):68-71.
115. Bootman MD, Rietdorf K, Collins T, Walker S, Sanderson M. Ca2+-sensitive fluorescent dyes and intracellular Ca2+ imaging. Cold Spring Harb Protoc. 2013;2013(2):83-99.
116. Grynkiewicz G, Poenie M, Tsien RY. A New Generation of Ca-2+ Indicators with Greatly Improved Fluorescence Properties. J Biol Chem. 1985;260(6):3440-50.
117. Minta A, Kao JPY, Tsien RY. Fluorescent Indicators for Cytosolic Calcium Based on Rhodamine and Fluorescein Chromophores. J Biol Chem. 1989;264(14):8171-8.
118. Flagmeier P, De S, Wirthensohn DC, Lee SF, Vincke C, Muyldermans S, et al. Ultrasensitive measurement of Ca2+ influx into lipid vesicles induced by protein aggregates. Eur Biophys J Biophy. 2017;46:S237-S.
119. De S, Wirthensohn DC, Flagmeier P, Hughes C, Aprile FA, Ruggeri FS, et al. Different soluble aggregates of A beta 42 can give rise to cellular toxicity through different mechanisms. Nat Commun. 2019;10.
120. Davies M, Jung C, Wallis P, Schnitzler T, Li C, Mullen K, et al. Photophysics of new photostable rylene derivatives: applications in single-molecule studies and membrane labelling. Chemphyschem. 2011;12(8):1588-95.
121. Chien MH, Brameshuber M, Rossboth BK, Schutz GJ, Schmid S. Single-molecule optical absorption imaging by nanomechanical photothermal sensing. Proc Natl Acad Sci U S A. 2018;115(44):11150-5.
122. Korlacki R, Steiner M, Qian H, Hartschuh A, Meixner AJ. Optical Fourier transform spectroscopy of single-walled carbon nanotubes and single molecules. Chemphyschem. 2007;8(7):1049-55.
123. Sun M, Mullen K, Yin M. Water-soluble perylenediimides: design concepts and biological applications. Chem Soc Rev. 2016;45(6):1513-28.
124. Vakuliuk O, Jun YW, Vygranenko K, Clermont G, Reo YJ, Blanchard-Desce M, et al. Modified Isoindolediones as Bright Fluorescent Probes for Cell and Tissue Imaging. Chemistry. 2019;25(58):13354-62.
125. Kaur M, Choi DH. Diketopyrrolopyrrole: brilliant red pigment dye-based fluorescent probes and their applications. Chem Soc Rev. 2015;44(1):58-77.
126. Wang J, Xu W, Yang Z, Yan Y, Xie X, Qu N, et al. New Diketopyrrolopyrrole-Based Ratiometric Fluorescent Probe for Intracellular Esterase Detection and Discrimination of Live and Dead Cells in Different Fluorescence Channels. ACS Appl Mater Interfaces. 2018;10(37):31088-95.
127. Shimomura O, Johnson FH, Saiga Y. Extraction, purification and properties of aequorin, a bioluminescent protein from the luminous hydromedusan, Aequorea. J Cell Comp Physiol. 1962;59:223-39.
128. Lenn T, Leake MC. Experimental approaches for addressing fundamental biological questions in living, functioning cells with single molecule precision. Open Biol. 2012;2.
129. Chiu SW, Leake MC. Functioning Nanomachines Seen in Real-Time in Living Bacteria Using Single-Molecule and Super-Resolution Fluorescence Imaging. Int J Mol Sci. 2011;12(4):2518-42.
130. Leake MC. Shining the spotlight on functional molecular complexes: The new science of single-molecule cell biology. Commun Integr Biol. 2010;3(5):415-8.
131. Bajar BT, Wang ES, Zhang S, Lin MZ, Chu J. A Guide to Fluorescent Protein FRET Pairs. Sensors (Basel). 2016;16(9).
132. Duncan RR. Fluorescence lifetime imaging microscopy (FLIM) to quantify protein-protein interactions inside cells. Biochem Soc Trans. 2006;34(Pt 5):679-82.
133. Koushik SV, Chen H, Thaler C, Puhl HL, 3rd, Vogel SS. Cerulean, Venus, and VenusY67C FRET reference standards. Biophys J. 2006;91(12):L99-L101.

134. Nenninger A, Mastroianni G, Robson A, Lenn T, Xue Q, Leake MC, et al. Independent mobility of proteins and lipids in the plasma membrane of Escherichia coli. Mol Microbiol. 2014;92(5):1142-53.
135. Griesbeck O, Baird GS, Campbell RE, Zacharias DA, Tsien RY. Reducing the environmental sensitivity of yellow fluorescent protein. Mechanism and applications. J Biol Chem. 2001;276(31):29188-94.
136. Shaner NC, Steinbach PA, Tsien RY. A guide to choosing fluorescent proteins. Nat Methods. 2005;2(12):905-9.
137. Bajar BT, Wang ES, Lam AJ, Kim BB, Jacobs CL, Howe ES, et al. Improving brightness and photostability of green and red fluorescent proteins for live cell imaging and FRET reporting. Sci Rep. 2016;6:20889.
138. Esposito A, Gralle M, Dani MA, Lange D, Wouters FS. pHlameleons: a family of FRET-based protein sensors for quantitative pH imaging. Biochemistry. 2008;47(49):13115-26.
139. Tsutsui H, Karasawa S, Okamura Y, Miyawaki A. Improving membrane voltage measurements using FRET with new fluorescent proteins. Nat Methods. 2008;5(8):683-5.
140. George Abraham B, Sarkisyan KS, Mishin AS, Santala V, Tkachenko NV, Karp M. Fluorescent Protein Based FRET Pairs with Improved Dynamic Range for Fluorescence Lifetime Measurements. Plos One. 2015;10(8):e0134436.
141. Sarkisyan KS, Goryashchenko AS, Lidsky PV, Gorbachev DA, Bozhanova NG, Gorokhovatsky AY, et al. Green fluorescent protein with anionic tryptophan-based chromophore and long fluorescence lifetime. Biophys J. 2015;109(2):380-9.
142. Wang L, Jackson WC, Steinbach PA, Tsien RY. Evolution of new nonantibody proteins via iterative somatic hypermutation. Proc Natl Acad Sci U S A. 2004;101(48):16745-9.
143. Lukyanov KA, Chudakov DM, Lukyanov S, Verkhusha VV. Innovation: Photoactivatable fluorescent proteins. Nat Rev Mol Cell Biol. 2005;6(11):885-91.
144. Plank M, Wadhams GH, Leake MC. Millisecond timescale slimfield imaging and automated quantification of single fluorescent protein molecules for use in probing complex biological processes. Integr Biol-Uk. 2009;1(10):602-12.
145. Bell AF, Stoner-Ma D, Wachter RM, Tonge PJ. Light-driven decarboxylation of wild-type green fluorescent protein. J Am Chem Soc. 2003;125(23):6919-26.
146. Chudakov DM, Verkhusha VV, Staroverov DB, Souslova EA, Lukyanov S, Lukyanov KA. Photoswitchable cyan fluorescent protein for protein tracking. Nat Biotechnol. 2004;22(11):1435-9.
147. Spencer SL, Cappell SD, Tsai FC, Overton KW, Wang CL, Meyer T. The proliferation-quiescence decision is controlled by a bifurcation in CDK2 activity at mitotic exit. Cell. 2013;155(2):369-83.
148. Regot S, Hughey JJ, Bajar BT, Carrasco S, Covert MW. High-sensitivity measurements of multiple kinase activities in live single cells. Cell. 2014;157(7):1724-34.
149. Resch-Genger U, Grabolle M, Cavaliere-Jaricot S, Nitschke R, Nann T. Quantum dots versus organic dyes as fluorescent labels. Nat Methods. 2008;5(9):763-75.
150. Chen O, Zhao J, Chauhan VP, Cui J, Wong C, Harris DK, et al. Compact high-quality CdSe-CdS core-shell nanocrystals with narrow emission linewidths and suppressed blinking. Nat Mater. 2013;12(5):445-51.
151. Dubertret B, Skourides P, Norris DJ, Noireaux V, Brivanlou AH, Libchaber A. In vivo imaging of quantum dots encapsulated in phospholipid micelles. Science. 2002;298(5599):1759-62.
152. Michalet X, Pinaud FF, Bentolila LA, Tsay JM, Doose S, Li JJ, et al. Quantum dots for live cells, in vivo imaging, and diagnostics. Science. 2005;307(5709):538-44.
153. Wegner KD, Hildebrandt N. Quantum dots: bright and versatile in vitro and in vivo fluorescence imaging biosensors. Chem Soc Rev. 2015;44(14):4792-834.
154. Baba K, Nishida K. Single-molecule tracking in living cells using single quantum dot applications. Theranostics. 2012;2(7):655-67.

155. Amelia M, Lincheneau C, Silvi S, Credi A. Electrochemical properties of CdSe and CdTe quantum dots. Chem Soc Rev. 2012;41(17):5728-43.
156. Cui L, Li CC, Tang B, Zhang CY. Advances in the integration of quantum dots with various nanomaterials for biomedical and environmental applications. Analyst. 2018;143(11):2469-78.
157. Bera D, Qian L, Tseng TK, Holloway PH. Quantum Dots and Their Multimodal Applications: A Review. Materials. 2010;3(4):2260-345.
158. Valizadeh A, Mikaeili H, Samiei M, Farkhani SM, Zarghami N, Kouhi M, et al. Quantum dots: synthesis, bioapplications, and toxicity. Nanoscale Res Lett. 2012;7(1):480.
159. Sundara Rajan S, Vu TQ. Quantum dots monitor TrkA receptor dynamics in the interior of neural PC12 cells. Nano Lett. 2006;6(9):2049-59.
160. Hohng S, Ha T. Single-molecule quantum-dot fluorescence resonance energy transfer. Chemphyschem. 2005;6(5):956-60.
161. Fonthal G, Tirado-Mejia L, Marin-Hurtado JI, Ariza-Calderon H, Mendoza-Alvarez JG. Temperature dependence of the band gap energy of crystalline CdTe. J Phys Chem Solids. 2000;61(4):579-83.
162. Petryayeva E, Algar WR, Medintz IL. Quantum Dots in Bioanalysis: A Review of Applications Across Various Platforms for Fluorescence Spectroscopy and Imaging. Appl Spectrosc. 2013;67(3):215-52.
163. Mo YM, Tang Y, Gao F, Yang J, Zhang YM. Synthesis of Fluorescent CdS Quantum Dots of Tunable Light Emission with a New in Situ Produced Capping Agent. Ind Eng Chem Res. 2012;51(17):5995-6000.
164. Wei CJ, Li JY, Gao F, Guo SX, Zhou YC, Zhao D. One-Step Synthesis of High-Quality Water-Soluble CdSe Quantum Dots Capped by N-Acetyl-L-cysteine via Hydrothermal Method and Their Characterization. J Spectrosc. 2015.
165. Yao J, Li L, Li P, Yang M. Quantum dots: from fluorescence to chemiluminescence, bioluminescence, electrochemiluminescence, and electrochemistry. Nanoscale. 2017;9(36):13364-83.
166. Yu WW, Qu LH, Guo WZ, Peng XG. Experimental determination of the extinction coefficient of CdTe, CdSe, and CdS nanocrystals. Chem Mater. 2003;15(14):2854-60.
167. Gao XH, Cui YY, Levenson RM, Chung LWK, Nie SM. In vivo cancer targeting and imaging with semiconductor quantum dots. Nature Biotechnology. 2004;22(8):969-76.
168. Voura EB, Jaiswal JK, Mattoussi H, Simon SM. Tracking metastatic tumor cell extravasation with quantum dot nanocrystals and fluorescence emission-scanning microscopy. Nat Med. 2004;10(9):993-8.
169. Vu TQ, Lam WY, Hatch EW, Lidke DS. Quantum dots for quantitative imaging: from single molecules to tissue. Cell Tissue Res. 2015;360(1):71-86.
170. Quinn SD, Magennis SW. Optical detection of gadolinium(III) ions via quantum dot aggregation. Rsc Adv. 2017;7(40):24730-5.
171. Quinn SD, Rafferty A, Dick E, Morten MJ, Kettles FJ, Knox C, et al. Surface Charge Control of Quantum Dot Blinking. J Phys Chem C. 2016;120(34):19487-91.
172. Umakoshi T, Udaka H, Uchihashi T, Ando T, Suzuki M, Fukuda T. Quantum-dot antibody conjugation visualized at the single-molecule scale with high-speed atomic force microscopy. Colloid Surface B. 2018;167:267-74.
173. Deerinck TJ. The Application of Fluorescent Quantum Dots to Confocal, Multiphoton, and Electron Microscopic Imaging. Toxicol Pathol. 2008;36(1):112-6.
174. Ebenstein Y, Mokari T, Banin U. Fluorescence quantum yield of CdSe/ZnS nanocrystals investigated by correlated atomic-force and single-particle fluorescence microscopy. Appl Phys Lett. 2002;80(21):4033-5.
175. Wagner AM, Knipe JM, Orive G, Peppas NA. Quantum dots in biomedical applications. Acta Biomater. 2019;94:44-63.

176. Zhang X, Zhang B, Miao WJ, Zou GZ. Molecular-Counting-Free and Electrochemiluminescent Single-Molecule Immunoassay with Dual-Stabilizers-Capped CdSe Nanocrystals as Labels. Anal Chem. 2016;88(10):5482-8.
177. Li MY, Sun YM, Chen L, Li L, Zou GZ, Zhang XL, et al. Ultrasensitive Eletrogenerated Chemiluminescence Immunoassay by Magnetic Nanobead Amplification. Electroanal. 2010;22(3):333-7.
178. Dahan M, Levi S, Luccardini C, Rostaing P, Riveau B, Triller A. Diffusion dynamics of glycine receptors revealed by single-quantum dot tracking. Science. 2003;302(5644):442-5.
179. Cui BX, Wu CB, Chen L, Ramirez A, Bearer EL, Li WP, et al. One at a time, live tracking of NGF axonal transport using quantum dots. P Natl Acad Sci USA. 2007;104(34):13666-71.
180. Pinaud F, Michalet X, Iyer G, Margeat E, Moore HP, Weiss S. Dynamic Partitioning of a Glycosyl-Phosphatidylinositol-Anchored Protein in Glycosphingolipid-Rich Microdomains Imaged by Single-Quantum Dot Tracking. Traffic. 2009;10(6):691-712.
181. Murcia MJ, Minner DE, Mustata GM, Ritchie K, Naumann CA. Design of Quantum Dot-Conjugated Lipids for Long-Term, High-Speed Tracking Experiments on Cell Surfaces. J Am Chem Soc. 2008;130(45):15054-62.
182. Tada H, Higuchi H, Wanatabe TM, Ohuchi N. In vivo real-time tracking of single quantum dots conjugated with monoclonal anti-HER2 antibody in tumors of mice. Cancer Res. 2007;67(3):1138-44.
183. Zhang Q, Li YL, Tsien RW. The Dynamic Control of Kiss-And-Run and Vesicular Reuse Probed with Single Nanoparticles. Science. 2009;323(5920):1448-53.
184. Smith CS, Joseph N, Rieger B, Lidke KA. Fast, single-molecule localization that achieves theoretically minimum uncertainty. Nat Methods. 2010;7(5):373-U52.
185. Owens J, Brus L. Chemical Synthesis and Luminescence Applications of Colloidal Semiconductor Quantum Dots. J Am Chem Soc. 2017;139(32):10939-43.
186. Kovalenko MV, Manna L, Cabot A, Hens Z, Talapin DV, Kagan CR, et al. Prospects of Nanoscience with Nanocrystals. Acs Nano. 2015;9(2):1012-57.
187. Zhan NQ, Palui G, Mattoussi H. Preparation of compact biocompatible quantum dots using multicoordinating molecular-scale ligands based on a zwitterionic hydrophilic motif and lipoic acid anchors. Nat Protoc. 2015;10(6):859-74.
188. Chang JC, Rosenthal SJ. Quantum dot-based single-molecule microscopy for the study of protein dynamics. Methods Mol Biol. 2013;1026:71-84.
189. Farlow J, Seo D, Broaders KE, Taylor MJ, Gartner ZJ, Jun YW. Formation of targeted monovalent quantum dots by steric exclusion. Nat Methods. 2013;10(12):1203-5.
190. Bhatia D, Arumugam S, Nasilowski M, Joshi H, Wunder C, Chambon V, et al. Quantum dot-loaded monofunctionalized DNA icosahedra for single-particle tracking of endocytic pathways. Nat Nanotechnol. 2016;11(12):1112-9.
191. Smith AM, Nie S. Compact quantum dots for single-molecule imaging. J Vis Exp. 2012(68).
192. Zhou J, Liu Y, Tang J, Tang WH. Surface ligands engineering of semiconductor quantum dots for chemosensory and biological applications. Mater Today. 2017;20(7):360-76.
193. Tang B, Liu BH, Liu ZY, Luo MY, Shi XH, Pang DW. Quantum Dots with a Compact Amphiphilic Zwitterionic Coating. ACS Appl Mater Interfaces. 2022;14(24):28097-104.
194. Bruchez MP. Quantum dots find their stride in single molecule tracking. Current Opinion in Chemical Biology. 2011;15(6):775-80.
195. Clarke S, Pinaud F, Beutel O, You C, Piehler J, Dahan M. Covalent monofunctionalization of peptide-coated quantum dots for single-molecule assays. Nano Lett. 2010;10(6):2147-54.
196. Zhang YJ, Clapp A. Overview of Stabilizing Ligands for Biocompatible Quantum Dot Nanocrystals. Sensors-Basel. 2011;11(12):11036-55.
197. Wagner AM, Knipe JM, Orive G, Peppas NA. Quantum dots in biomedical applications. Acta Biomater. 2019;94:44-63.

198. Galland C, Ghosh Y, Steinbruck A, Sykora M, Hollingsworth JA, Klimov VI, et al. Two types of luminescence blinking revealed by spectroelectrochemistry of single quantum dots. Nature. 2011;479(7372):203-7.
199. Nagao Y, Fujiwara H, Sasaki K. Analysis of Trap-State Dynamics of Single CdSe/ZnS Quantum Dots on a TiO2 Substrate with Different Nb Concentrations. J Phys Chem C. 2014;118(35):20571-5.
200. Lidke K, Rieger B, Jovin T, Heintzmann R. Superresolution by localization of quantum dots using blinking statistics. Opt Express. 2005;13(18):7052-62.
201. Hardman R. A toxicologic review of quantum dots: Toxicity depends on physicochemical and environmental factors. Environ Health Persp. 2006;114(2):165-72.
202. Hohng S, Ha T. Near-complete suppression of quantum dot blinking in ambient conditions. J Am Chem Soc. 2004;126(5):1324-5.
203. Oh E, Liu R, Nel A, Gemill KB, Bilal M, Cohen Y, et al. Meta-analysis of cellular toxicity for cadmium-containing quantum dots. Nat Nanotechnol. 2016;11(5):479-86.
204. Tsoi KM, Dai Q, Alman BA, Chan WC. Are quantum dots toxic? Exploring the discrepancy between cell culture and animal studies. Acc Chem Res. 2013;46(3):662-71.
205. Winnik FM, Maysinger D. Quantum dot cytotoxicity and ways to reduce it. Acc Chem Res. 2013;46(3):672-80.
206. Matos B, Martins M, Samamed AC, Sousa D, Ferreira I, Diniz MS. Toxicity Evaluation of Quantum Dots (ZnS and CdS) Singly and Combined in Zebrafish (Danio rerio). Int J Environ Res Public Health. 2019;17(1).
207. Shenderova O, Nunn N, Oeckinghaus T, Torelli M, McGuire G, Smith K, et al. Commercial quantities of ultrasmall fluorescent nanodiamonds containing color centers. Proc Spie. 2017;10118.
208. Liu KK, Cheng CL, Chang CC, Chao JI. Biocompatible and detectable carboxylated nanodiamond on human cell. Nanotechnology. 2007;18(32).
209. Schrand AM, Huang HJ, Carlson C, Schlager JJ, Osawa E, Hussain SM, et al. Are diamond nanoparticles cytotoxic? J Phys Chem B. 2007;111(1):2-7.
210. Alkahtani MH, Alghannam F, Jiang L, Almethen A, Rampersaud AA, Brick R, et al. Fluorescent nanodiamonds: past, present, and future. Nanophotonics-Berlin. 2018;7(8):1423-53.
211. Hsiao WW, Hui YY, Tsai PC, Chang HC. Fluorescent Nanodiamond: A Versatile Tool for Long-Term Cell Tracking, Super-Resolution Imaging, and Nanoscale Temperature Sensing. Acc Chem Res. 2016;49(3):400-7.
212. Reineck P, Francis A, Orth A, Lau DWM, Nixon-Luke RDV, Das Rastogi I, et al. Brightness and Photostability of Emerging Red and Near-IR Fluorescent Nanomaterials for Bioimaging. Adv Opt Mater. 2016;4(10):1549-57.
213. Schirhagl R, Chang K, Loretz M, Degen CL. Nitrogen-Vacancy Centers in Diamond: Nanoscale Sensors for Physics and Biology. Annual Review of Physical Chemistry, Vol 65. 2014;65:83-105.
214. Wu YZ, Jelezko F, Plenio MB, Weil T. Diamond Quantum Devices in Biology. Angew Chem Int Edit. 2016;55(23):6586-98.
215. Iwasaki T, Miyamoto Y, Taniguchi T, Siyushev P, Metsch MH, Jelezko F, et al. Tin-Vacancy Quantum Emitters in Diamond. Phys Rev Lett. 2017;119(25).
216. Balasubramanian G, Chan IY, Kolesov R, Al-Hmoud M, Tisler J, Shin C, et al. Nanoscale imaging magnetometry with diamond spins under ambient conditions. Nature. 2008;455(7213):648-U46.
217. Rubio-Retama J, Hernando J, Lopez-Ruiz B, Hartl A, Steinmuller D, Stutzmann M, et al. Synthetic nanocrystalline diamond as a third-generation biosensor support. Langmuir. 2006;22(13):5837-42.
218. Hartl A, Schmich E, Garrido JA, Hernando J, Catharino SCR, Walter S, et al. Protein-modified nanocrystalline diamond thin films for biosensor applications. Nature Materials. 2004;3(10):736-42.
219. Yang WS, Auciello O, Butler JE, Cai W, Carlisle JA, Gerbi J, et al. DNA-modified nanocrystalline diamond thin-films as stable, biologically active substrates. Nature Materials. 2002;1(4):253-7.

220. Fu CC, Lee HY, Chen K, Lim TS, Wu HY, Lin PK, et al. Characterization and application of single fluorescent nanodiamonds as cellular biomarkers. P Natl Acad Sci USA. 2007;104(3):727-32.
221. Chang YR, Lee HY, Chen K, Chang CC, Tsai DS, Fu CC, et al. Mass production and dynamic imaging of fluorescent nanodiamonds. Nat Nanotechnol. 2008;3(5):284-8.
222. McGuinness LP, Yan Y, Stacey A, Simpson DA, Hall LT, Maclaurin D, et al. Quantum measurement and orientation tracking of fluorescent nanodiamonds inside living cells. Nat Nanotechnol. 2011;6(6):358-63.
223. Tisler J, Reuter R, Lammle A, Jelezko F, Balasubramanian G, Hemmer PR, et al. Highly Efficient FRET from a Single Nitrogen-Vacancy Center in Nanodiamonds to a Single Organic Molecule. Acs Nano. 2011;5(10):7893-8.
224. Kim YG, Ho SO, Gassman NR, Korlann Y, Landorf EV, Collart FR, et al. Efficient site-specific Labeling of proteins via cysteines. Bioconjugate Chem. 2008;19(3):786-91.
225. Ratner V, Kahana E, Eichler M, Haas E. A general strategy for site-specific double labeling of globular proteins for kinetic FRET studies. Bioconjugate Chem. 2002;13(5):1163-70.
226. Lee EM, Lee SS, Tripathi BN, Jung HS, Cao GP, Lee Y, et al. Site-directed mutagenesis substituting cysteine for serine in 2-Cys peroxiredoxin (2-Cys Prx A) of Arabidopsis thaliana effectively improves its peroxidase and chaperone functions. Ann Bot-London. 2015;116(4):713-25.
227. Kipper K, Eremina N, Marklund E, Tubasum S, Mao GZ, Lehmann LC, et al. Structure-guided approach to site-specific fluorophore labeling of the lac repressor LacI. Plos One. 2018;13(6).
228. Antia M, Islas LD, Boness DA, Baneyx G, Vogel V. Single molecule fluorescence studies of surface-adsorbed fibronectin. Biomaterials. 2006;27(5):679-90.
229. Puljung MC, Zagotta WN. Labeling of Specific Cysteines in Proteins Using Reversible Metal Protection. Biophys J. 2011;100(10):2513-21.
230. Amitani I, Liu BA, Dombrowski CC, Baskin RJ, Kowalczykowski SC. Watching Individual Proteins Acting on Single Molecules of DNA. Method Enzymol. 2010;472:261-91.
231. Galletto R, Amitani I, Baskin RJ, Kowalczykowski SC. Direct observation of individual RecA filaments assembling on single DNA molecules. Nature. 2006;443(7113):875-8.
232. Jakob L, Gust A, Grohmann D. Evaluation and optimisation of unnatural amino acid incorporation and bioorthogonal bioconjugation for site-specific fluorescent labelling of proteins expressed in mammalian cells. Biochem Biophys Rep. 2019;17:1-9.
233. Kim CH, Axup JY, Schultz PG. Protein conjugation with genetically encoded unnatural amino acids. Curr Opin Chem Biol. 2013;17(3):412-9.
234. Jewett JC, Sletten EM, Bertozzi CR. Rapid Cu-free click chemistry with readily synthesized biarylazacyclooctynones. J Am Chem Soc. 2010;132(11):3688-90.
235. Liu CC, Schultz PG. Adding New Chemistries to the Genetic Code. Annu Rev Biochem. 2010;79:413-44.
236. Liu WS, Brock A, Chen S, Chen SB, Schultz PG. Genetic incorporation of unnatural amino acids into proteins in mammalian cells. Nat Methods. 2007;4(3):239-44.
237. Benink HA, Urh M. HaloTag technology for specific and covalent labeling of fusion proteins. Methods Mol Biol. 2015;1266:119-28.
238. Tian H, Furstenberg A, Huber T. Labeling and Single-Molecule Methods To Monitor G Protein-Coupled Receptor Dynamics. Chem Rev. 2017;117(1):186-245.
239. Evans EGB, Millhauser GL. Genetic Incorporation of the Unnatural Amino Acid p-Acetyl Phenylalanine into Proteins for Site-Directed Spin Labeling. Electron Paramagnetic Resonance Investigations of Biological Systems by Using Spin Labels, Spin Probes, and Intrinsic Metal Ions, Pt A. 2015;563:503-27.
240. Tyagi S, Lemke EA. Genetically Encoded Click Chemistry for Single-Molecule FRET of Proteins. Laboratory Methods in Cell Biology: Imaging. 2012;113:169-87.
241. Brustad EM, Lemke EA, Schultz PG, Deniz AA. A General and Efficient Method for the Site-Specific Dual-Labeling of Proteins for Single Molecule Fluorescence Resonance Energy Transfer. J Am Chem Soc. 2008;130(52):17664-+.

242. Nikic-Spiegel I. Genetic Code Expansion- and Click Chemistry-Based Site-Specific Protein Labeling for Intracellular DNA-PAINT Imaging. Methods Mol Biol. 2018;1728:279-95.
243. Raulf A, Spahn CK, Zessin PJM, Finan K, Bernhardt S, Heckel A, et al. Click chemistry facilitates direct labelling and super-resolution imaging of nucleic acids and proteins. Rsc Adv. 2014;4(57):30462-6.
244. Pantoja R, Rodriguez EA, Dibas MI, Dougherty DA, Lester HA. Single-Molecule Imaging of a Fluorescent Unnatural Amino Acid Incorporated Into Nicotinic Receptors. Biophys J. 2009;96(1):226-37.
245. Hilairea MR, Ahmed IA, Lin CW, Jo H, DeGrado WF, Gai F. Blue fluorescent amino acid for biological spectroscopy and microscopy. P Natl Acad Sci USA. 2017;114(23):6005-9.
246. Summerer D, Chen S, Wu N, Deiters A, Chin JW, Schultz PG. A genetically encoded fluorescent amino acid. P Natl Acad Sci USA. 2006;103(26):9785-9.
247. Zhao M, Steffen FD, Borner R, Schaffer MF, Sigel RKO, Freisinger E. Site-specific dual-color labeling of long RNAs for single-molecule spectroscopy. Nucleic Acids Res. 2018;46(3).
248. Zohar H, Muller SJ. Labeling DNA for single-molecule experiments: methods of labeling internal specific sequences on double-stranded DNA. Nanoscale. 2011;3(8):3027-39.
249. Basu R, Lai LT, Meng ZY, Wu J, Shao FW, Zhang LF. Using Amino-Labeled Nucleotide Probes for Simultaneous Single Molecule RNA-DNA FISH. Plos One. 2014;9(9).
250. Chen X, Zhang D, Su N, Bao B, Xie X, Zuo F, et al. Visualizing RNA dynamics in live cells with bright and stable fluorescent RNAs. Nat Biotechnol. 2019;37(11):1287-93.
251. Sindbert S, Kalinin S, Hien N, Kienzler A, Clima L, Bannwarth W, et al. Accurate Distance Determination of Nucleic Acids via Forster Resonance Energy Transfer: Implications of Dye Linker Length and Rigidity. J Am Chem Soc. 2011;133(8):2463-80.
252. Pan KY, Boulais E, Yang L, Bathe M. Structure-based model for light-harvesting properties of nucleic acid nanostructures. Nucleic Acids Res. 2014;42(4):2159-70.
253. Dienerowitz M, Howard JAL, Quinn SD, Dienerowitz F, Leake MC. Single-molecule FRET dynamics of molecular motors in an ABEL trap. Methods. 2021;193:96-106.
254. Bornhorst JA, Falke JJ. Purification of proteins using polyhistidine affinity tags. Applications of Chimeric Genes and Hybrid Proteins, Pt A. 2000;326:245-54.
255. Lichty JJ, Malecki JL, Agnew HD, Michelson-Horowitz DJ, Tan S. Comparison of affinity tags for protein purification. Protein Expres Purif. 2005;41(1):98-105.
256. Li YF. Commonly used tag combinations for tandem affinity purification. Biotechnol Appl Bioc. 2010;55:73-83.
257. Cole NB. Site-specific protein labeling with SNAP-tags. Curr Protoc Protein Sci. 2013;73:Unit 30 1.
258. Quinn SD, Srinivasan S, Gordon JB, He W, Carraway KL, Coleman MA, et al. Single-Molecule Fluorescence Detection of the Epidermal Growth Factor Receptor in Membrane Discs. Biochemistry. 2019;58(4):286-94.
259. Srinivasan S, Regmi R, Lin X, Dreyer CA, Chen X, Quinn SD, et al. Ligand-induced transmembrane conformational coupling in monomeric EGFR. Nat Commun. 2022;13(1):3709.
260. Hinner MJ, Johnsson K. How to obtain labeled proteins and what to do with them. Curr Opin Biotech. 2010;21(6):766-76.
261. Srikun D, Albers AE, Nam CI, Iavaron AT, Chang CJ. Organelle-Targetable Fluorescent Probes for Imaging Hydrogen Peroxide in Living Cells via SNAP-Tag Protein Labeling. J Am Chem Soc. 2010;132(12):4455-65.
262. Klein T, Loschberger A, Proppert S, Wolter S, van de Linde SV, Sauer M. Live-cell dSTORM with SNAP-tag fusion proteins. Nat Methods. 2011;8(1):7-9.
263. Bojkowska K, de Sio FS, Barde I, Offner S, Verp S, Heinis C, et al. Measuring In Vivo Protein Half-Life. Chem Biol. 2011;18(6):805-15.

264. Ville D, de Bellescize J, Nguyen MA, Testard H, Gautier A, Perrier J, et al. Ring 14 chromosome presenting as early-onset isolated partial epilepsy. Dev Med Child Neurol. 2009;51(11):917-22.
265. Zhang CJ, Li L, Chen GYJ, Xu QH, Yao SQ. One- and Two-Photon Live Cell Imaging Using a Mutant SNAP-Tag Protein and Its FRET Substrate Pairs. Org Lett. 2011;13(16):4160-3.
266. Calebiro D, Rieken F, Wagner J, Sungkaworn T, Zabel U, Borzi A, et al. Single-molecule analysis of fluorescently labeled G-protein-coupled receptors reveals complexes with distinct dynamics and organization. P Natl Acad Sci USA. 2013;110(2):743-8.
267. Los GV, Encell LP, McDougall MG, Hartzell DD, Karassina N, Zimprich C, et al. HaloTag: a novel protein labeling technology for cell imaging and protein analysis. Acs Chem Biol. 2008;3(6):373-82.
268. Popa I, Berkovich R, Alegre-Cebollada J, Badilla CL, Rivas-Pardo JA, Taniguchi Y, et al. Nanomechanics of HaloTag tethers. J Am Chem Soc. 2013;135(34):12762-71.
269. England CG, Luo H, Cai W. HaloTag technology: a versatile platform for biomedical applications. Bioconjug Chem. 2015;26(6):975-86.
270. Hoffmann C, Gaietta G, Zurn A, Adams SR, Terrillon S, Ellisman MH, et al. Fluorescent labeling of tetracysteine-tagged proteins in intact cells. Nat Protoc. 2010;5(10):1666-77.
271. Gelman H, Wirth AJ, Gruebele M. ReAsH as a Quantitative Probe of In-Cell Protein Dynamics. Biochemistry. 2016;55(13):1968-76.
272. Fernandes DD, Bamrah J, Kailasam S, Gomes GW, Li Y, Wieden HJ, et al. Characterization of Fluorescein Arsenical Hairpin (FlAsH) as a Probe for Single-Molecule Fluorescence Spectroscopy. Sci Rep. 2017;7(1):13063.
273. Shimogawa M, Petersson EJ. New strategies for fluorescently labeling proteins in the study of amyloids. Curr Opin Chem Biol. 2021;64:57-66.
274. Bernas T, Zarebski M, Cook PR, Dobrucki JW. Minimizing photobleaching during confocal microscopy of fluorescent probes bound to chromatin: role of anoxia and photon flux (vol 215, pg 281, 2004). J Microsc-Oxford. 2004;216:197-.
275. Sabir T, Toulmin A, Ma L, Jones AC, McGlynn P, Schroder GF, et al. Branchpoint Expansion in a Fully Complementary Three-Way DNA Junction. J Am Chem Soc. 2012;134(14):6280-5.
276. Basche T, Kummer S, Brauchle C. Direct Spectroscopic Observation of Quantum Jumps of a Single-Molecule. Nature. 1995;373(6510):132-4.
277. Kondo T, Pinnola A, Chen WJ, Dall'Osto L, Bassi R, Schlau-Cohen GS. Single-molecule spectroscopy of LHCSR1 protein dynamics identifies two distinct states responsible for multi-timescale photosynthetic photoprotection. Nat Chem. 2017;9(8):772-8.
278. Cordes T, Vogelsang J, Tinnefeld P. On the Mechanism of Trolox as Antiblinking and Antibleaching Reagent. J Am Chem Soc. 2009;131(14):5018-+.
279. Frigault MM, Lacoste J, Swift JL, Brown CM. Live-cell microscopy - tips and tools. J Cell Sci. 2009;122(6):753-67.
280. Waters JC. Live-Cell Fluorescence Imaging. Digital Microscopy, 4th Edition. 2013;114:125-50.
281. Bogdanov AM, Kudryavtseva EI, Lukyanov KA. Anti-fading media for live cell GFP imaging. Plos One. 2012;7(12):e53004.
282. Hohng S, Ha T. Near-complete suppression of quantum dot blinking in ambient conditions. J Am Chem Soc. 2004;126(5):1324-5.
283. Li B, Zhang G, Wang Z, Li Z, Chen R, Qin C, et al. Suppressing the Fluorescence Blinking of Single Quantum Dots Encased in N-type Semiconductor Nanoparticles. Sci Rep. 2016;6:32662.
284. Renikuntla BR, Rose HC, Eldo J, Waggoner AS, Armitage BA. Improved photostability and fluorescence properties through polyfluorination of a cyanine dye. Org Lett. 2004;6(6):909-12.
285. Funabiki K, Saito Y, Kikuchi T, Yagi K, Kubota Y, Inuzuka T, et al. Aromatic Fluorine-Induced One-Pot Synthesis of Ring-Perfluorinated Trimethine Cyanine Dye and Its Remarkable Fluorescence Properties. J Org Chem. 2019;84(7):4372-80.

286. Zheng Q, Lavis LD. Development of photostable fluorophores for molecular imaging. Curr Opin Chem Biol. 2017;39:32-8.
287. Zheng QS, Jockusch S, Rodriguez-Calero GG, Zhou Z, Zhao H, Altman RB, et al. Intra-molecular triplet energy transfer is a general approach to improve organic fluorophore photostability. Photoch Photobio Sci. 2016;15(2):196-203.
288. Shao N, Qi Y, Lu H, He D, Li B, Huang Y. Photostability Highly Improved Nanoparticles Based on IR-780 and Negative Charged Copolymer for Enhanced Photothermal Therapy. ACS Biomater Sci Eng. 2019;5(2):795-804.
289. Jiao L, Song F, Zhang B, Ning H, Cui J, Peng X. Improving the brightness and photostability of NIR fluorescent silica nanoparticles through rational fine-tuning of the covalent encapsulation methods. J Mater Chem B. 2017;5(26):5278-83.
290. Bera A, Bagchi D, Pal SK. Improvement of Photostability and NIR Activity of Cyanine Dye through Nanohybrid Formation: Key Information from Ultrafast Dynamical Studies. J Phys Chem A. 2019;123(35):7550-7.
291. Dresser L, Hunter P, Yendybayeva F, Hargreaves AL, Howard JAL, Evans GJO, et al. Amyloid-beta oligomerization monitored by single-molecule stepwise photobleaching. Methods. 2021;193:80-95.
292. Grubetamayer KS, Yserentant K, Herten DP. Photons in - numbers out: perspectives in quantitative fluorescence microscopy for in situ protein counting. Methods Appl Fluoresc. 2019;7(1):012003.
293. Redy-Keisar O, Huth K, Vogel U, Lepenies B, Seeberger PH, Haag R, et al. Enhancement of fluorescent properties of near-infrared dyes using clickable oligoglycerol dendrons. Org Biomol Chem. 2015;13(16):4727-32.
294. van Oijen AM. Single-molecule approaches to characterizing kinetics of biomolecular interactions. Curr Opin Biotech. 2011;22(1):75-80.
295. Sisamakis E, Valeri A, Kalinin S, Rothwell PJ, Seidel CAM. Accurate Single-Molecule Fret Studies Using Multiparameter Fluorescence Detection. Methods in Enzymology, Vol 475: Single Molecule Tools, Pt B. 2010;475:455-514.
296. Eilers Y, Ta H, Gwosch KC, Balzarotti F, Hell SW. MINFLUX monitors rapid molecular jumps with superior spatiotemporal resolution. P Natl Acad Sci USA. 2018;115(24):6117-22.
297. Schermelleh L, Ferrand A, Huser T, Eggeling C, Sauer M, Biehlmaier O, et al. Super-resolution microscopy demystified. Nat Cell Biol. 2019;21(1):72-84.
298. Shashkova S, Leake MC. Single-molecule fluorescence microscopy review: shedding new light on old problems. Bioscience Rep. 2017;37.
299. Walter NG, Huang CY, Manzo AJ, Sobhy MA. Do-it-yourself guide: how to use the modern single-molecule toolkit. Nature Methods. 2008;5(6):475-89.
300. Aleman EA, Pedini HS, Rueda D. Covalent-Bond-Based Immobilization Approaches for Single-Molecule Fluorescence. Chembiochem. 2009;10(18):2862-6.
301. Okumus B, Wilson TJ, Lilley DMJ, Ha T. Vesicle encapsulation studies reveal that single molecule ribozyme heterogeneities are intrinsic. Biophys J. 2004;87(4):2798-806.
302. Hong CA, Son HY, Nam YS. Layer-by-layer siRNA/poly(L-lysine) Multilayers on Polydopamine-coated Surface for Efficient Cell Adhesion and Gene Silencing. Sci Rep-Uk. 2018;8.
303. Dickson RM, Cubitt AB, Tsien RY, Moerner WE. On/off blinking and switching behaviour of single molecules of green fluorescent protein. Nature. 1997;388(6640):355-8.
304. Ray K, Ma JX, Oram M, Lakowicz JR, Black LW. Single-Molecule and FRET Fluorescence Correlation Spectroscopy Analyses of Phage DNA Packaging: Colocalization of Packaged Phage T4 DNA Ends within the Capsid. J Mol Biol. 2010;395(5):1102-13.
305. Elson EL. Fluorescence correlation spectroscopy: past, present, future. Biophys J. 2011;101(12):2855-70.
306. Robson A, Burrage K, Leake MC. Inferring diffusion in single live cells at the single-molecule level. Philos T R Soc B. 2013;368(1611).

307. Xue Q, Leake MC. A Novel Multiple Particle Tracking Algorithm for Noisy in Vivo Data by Minimal Path Optimization within the Spatio-Temporal Volume. 2009 Ieee International Symposium on Biomedical Imaging: From Nano to Macro, Vols 1 and 2. 2009:1158-61.
308. Xue QA, Jones NS, Leake MC. A General Approach for Segmenting Elongated and Stubby Biological Objects: Extending a Chord Length Transform with the Radon Transform. I S Biomed Imaging. 2010:161-4.
309. Wilson LG, Carter LM, Reece SE. High-speed holographic microscopy of malaria parasites reveals ambidextrous flagellar waveforms. P Natl Acad Sci USA. 2013;110(47):18769-74.
310. Ortega-Arroyo J, Kukura P. Interferometric scattering microscopy (iSCAT): new frontiers in ultrafast and ultrasensitive optical microscopy. Phys Chem Chem Phys. 2012;14(45):15625-36.
311. Wollman AJM, Miller H, Foster S, Leake MC. An automated image analysis framework for segmentation and division plane detection of single live Staphylococcus aureus cells which can operate at millisecond sampling time scales using bespoke Slimfield microscopy. Phys Biol. 2016;13(5).
312. Manley S, Gillette JM, Patterson GH, Shroff H, Hess HF, Betzig E, et al. High-density mapping of single-molecule trajectories with photoactivated localization microscopy. Nat Methods. 2008;5(2):155-7.
313. Ha T, Tinnefeld P. Photophysics of fluorescent probes for single-molecule biophysics and super-resolution imaging. Annu Rev Phys Chem. 2012;63:595-617.
314. Dempsey GT, Vaughan JC, Chen KH, Bates M, Zhuang XW. Evaluation of fluorophores for optimal performance in localization-based super-resolution imaging. Nature Methods. 2011;8(12):1027-+.
315. Fernandez-Suarez M, Ting AY. Fluorescent probes for super-resolution imaging in living cells. Nat Rev Mol Cell Bio. 2008;9(12):929-43.
316. Zou Z, Luo ZL, Xu X, Yang S, Qing ZH, Liu JW, et al. Photoactivatable fluorescent probes for spatiotemporal-controlled biosensing and imaging. Trac-Trend Anal Chem. 2020;125.
317. Banaz N, Makela J, Uphoff S. Choosing the right label for single-molecule tracking in live bacteria: side-by-side comparison of photoactivatable fluorescent protein and Halo tag dyes. J Phys D Appl Phys. 2019;52(6):064002.